Science of the Total Environment 903 (2023) 166103

Contents lists available at ScienceDirect

Science of the Total Environment

journal homepage: www.elsevier.com/locate/scitotenv

River widening in mountain and foothill areas during floods: Insights from a meta-analysis of 51 European Rivers

V. Ruiz-Villanueva [a,*], H. Piégay [b], Vittoria Scorpio [c], Annette Bachmann [d], Guillaume Brousse [e], Marco Cavalli [f], Francesco Comiti [g], Stefano Crema [f], Elena Fernández [h], Glòria Furdada [i], Hanna Hajdukiewicz [j], Lukas Hunzinger [d], Ana Lucía [k], Lorenzo Marchi [f], Adina Moraru [l], Guillaume Piton [m], Dieter Rickenmann [n], Margherita Righini [o], Nicola Surian [p], Rabab Yassine [q], Bartłomiej Wyżga [j]

[a] University of Lausanne, Institute of Earth Surface Dynamics (IDYST), Geopolis, UNIL-Mouline, CH-1015 Lausanne, Switzerland
[b] École Normale Supérieure de Lyon, (ENS), France, Environment City Society (EVS) Research unit, UMR 5600, 15 parvis René Descartes, 69342 Lyon, France
[c] Department of Chemical and Geological Sciences, University of Modena and Reggio Emilia, Modena, Italy
[d] Flussbau AG SAH, Schwarztorstrasse 7, 3007 Bern, Switzerland
[e] EDF – R&D – LNHE - 6 Quai Watier, Chatou/Laboratoire d'Hydraulique Saint-Venant - 6 Quai Watier, 78400 Chatou, France
[f] National Research Council, Research Institute for Geo-Hydrological Protection (CNR IRPI), Corso Stati Uniti 4, 35127 Padova, Italy
[g] Free University of Bolzano-Bozen, Faculty of Science and Technology, Bolzano, Italy
[h] INDUROT, University of Oviedo, 33600 Mieres, Asturias, Spain
[i] RISKNAT Research group, Geomodels Research Institute, Universitat de Barcelona, UB (Spain), Departament de Dinàmica de la Terra i de l'Oceà, Facultat de Ciències de la Terra, c/Martí i Franquès s/n, 08028 Barcelona, Spain
[j] Institute of Nature Conservation, Polish Academy of Sciences, al. Mickiewicza 33, 31-120 Kraków, Poland
[k] Geological and Mining Institute of Spain, National Research Council (IGME-CSIC), Ríos Rosas 23, 28003 Madrid, Spain
[l] Norwegian University of Science and Technology, (NTNU) Department of Civil and Environmental Engineering, S.P. Andersens veg 5, 7031 Trondheim, Norway
[m] Univ. Grenoble Alpes, INRAE, CNRS, IRD, Grenoble INP, IGE, 38000 Grenoble, France
[n] Swiss Federal Research Institute WSL, Zürcherstrasse 111, CH-8903 Birmensdorf, Switzerland
[o] IUSS - University School for Advanced Studies, 15, 27100 Pavia, Italy
[p] University of Padova, Department of Geosciences, Via G. Gradenigo 6, 35131 Padova, Italy
[q] EGIS 889 rue de la Vielle Poste CS, Montpellier 34965, France

HIGHLIGHTS

- We show how different types of rivers responded to floods in terms of channel widening.
- Mediterranean rivers experienced the largest widening.
- We identified which floods and morphological variables were responsible for widening.
- We proposed new statistical models to predict channel widening.

GRAPHICAL ABSTRACT

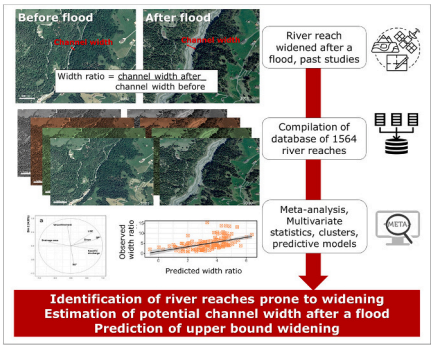

* Corresponding author.
E-mail address: Virginia.Ruiz-Villanueva@unil.ch (V. Ruiz-Villanueva).

https://doi.org/10.1016/j.scitotenv.2023.166103
Received 22 May 2023; Received in revised form 17 July 2023; Accepted 5 August 2023
Available online 7 August 2023

ARTICLE INFO

Editor: Fernando A.L. Pacheco

Keywords:
Bank erosion
Width ratio
Channel planform changes
Geomorphic changes
Flood response

ABSTRACT

River widening, defined as a lateral expansion of the channel, is a critical process that maintains fluvial ecosystems and is part of the regular functioning of rivers. However, in areas with high population density, channel widening can cause damage during floods. Therefore, for effective flood risk management it is essential to identify river reaches where abrupt channel widening may occur. Despite numerous efforts to predict channel widening, most studies have been limited to single rivers and single flood events, which may not be representative of other conditions. Moreover, a multi-catchment scale approach that covers various settings and flood magnitudes has been lacking. In this study, we fill this gap by compiling a large database comprising 1564 river reaches in several mountain regions in Europe affected by floods of varying magnitudes in the last six decades. By applying a meta-analysis, we aimed to identify the types of floods responsible for more extensive widening, the river reach types where intense widening is more likely to occur, and the hydraulic and morphological variables that explain widening and can aid in predicting widening. Our analysis revealed seven groups of reaches with significantly different responses to floods regarding width ratios (i.e., the ratio between channel width after and before a flood). Among these groups, the river reaches located in the Mediterranean region and affected by extreme floods triggered by short and intense precipitation events showed significantly larger widening than other river reaches in other regions. Additionally, the meta-analysis confirmed valley confinement as a critical morphological variable that controls channel widening but showed that it is not the only controlling factor. We proposed new statistical models to identify river reaches prone to widening, estimate potential channel width after a flood, and compute upper bound width ratios. These findings can inform flood hazard evaluations and the design of mitigation measures.

1. Introduction

River widening, defined as a lateral expansion of the channel width, is the dominant geomorphic response to floods (Magilligan et al., 2015), and an essential process that creates and maintains channel and floodplain complexity and sustains fluvial ecosystems (Hooke, 1979). Channel planform changes, including riverbank erosion and widening, provide multiple ecosystem benefits (Lawler, 1993), supplying sediment and large wood to the river network, and maintaining riparian diversity (Florsheim et al., 2008). These processes are positive phenomena that, where possible, need to be preserved (Piégay et al., 2005; Alber and Piégay, 2017) or in some cases, restored, as done by multiple European restoration strategies (Rohde et al., 2005; Beechie et al., 2010; Kline and Cahoon, 2010; Rohde et al., 2013; Biron et al., 2014; Buffin-Bélanger et al., 2015). However, in highly populated fluvial corridors, especially in mountain areas, channel widening can result in a loss of agricultural land and damage to infrastructures and buildings and, thus, it may be considered a natural hazard and a significant management aspect (Rickenmann et al., 2016; Comiti et al., 2016a). Indeed, in mountain streams, impacts of geomorphic processes (e.g., bed aggradation, channel widening) can be much more critical than inundation itself (Badoux et al., 2014; Rickenmann et al., 2016); still, river management rarely considers channel widening for flood mitigation (e.g., the EU Floods Directive, 2007/60/EC, neglects the analysis of planform changes).

River planform changes, including channel widening, may occur at various temporal and spatial scales. Feng et al. (2022) provided one of the first multi-decadal river extent changes at the global scale; however, most studies are regional or river specific (e.g., Surian et al., 2009; Arnaud et al., 2015; Scorpio et al., 2015; Hajdukiewicz et al., 2019). These longer-term studies focused on identifying trends and phases of channel narrowing and widening over several decades and attributed them to different drivers, such as flow regulation, in-channel gravel mining, or afforestation. Contrastingly, only some works addressed channel widening after single flood events. For example, the works by Buraas et al. (2014) and Magilligan et al. (2015) analysed the geomorphic signature of Tropical Storm Irene in 2011 on the White and the Saxtons Rivers in Vermont, or the study by Sholtes et al. (2018) along several streams impacted by the 2013 Colorado Front Range regional flood event, both in the US. Thompson and Croke (2013) and Fryirs et al. (2015) studied morphological changes along Lockyer Creek in southeast Queensland (Australia) after the flood in January 2011. More recently, Yousefi et al. (2018) explored the geomorphic changes after an extreme flood occurred in 2016 in the Karoon River in Iran. In Europe, several studies quantified geomorphic changes, including channel widening, after recent floods (e.g., Comiti et al., 2016b; Righini et al., 2017; Lucía et al., 2018; Ruiz-Villanueva et al., 2018; Scorpio et al., 2018). In these latter studies, channel widening was analysed using the width ratio (W_r), namely, the ratio between channel widths after and before the flood (Krapesch et al., 2011), and the authors identified the potential control variables that explained the observed W_r. We reviewed these previous works, focusing on European mountain and foothill rivers, and provided a summary of the main findings in Table 1 together with the equations proposed to predict the W_r.

All above-mentioned studies showed an extensive range of variability in terms of channel widening during floods, drivers might be site- and flood-specific, and the spatial scale (i.e., whether the analysis is done at the reach or the river scales) is very relevant (e.g., Krapesch et al., 2011). The researchers mentioned above proved that individual hydraulic variables alone do not entirely explain channel widening (e.g., Surian et al., 2016) and that the channel and basin features, such as valley confinement (Comiti et al., 2016b; Lucía et al., 2018), slope, sediment supply (Surian et al., 2016), and channel-bed type (bedrock or alluvial; Righini et al., 2017), also play important roles. The spatial distribution of precipitation and the generated peak discharges were found to be critical too (Ruiz-Villanueva et al., 2018; Scorpio et al., 2018), and other variables such as the forested channel length may also contribute (Ruiz-Villanueva et al., 2018). Despite the progress made in recent years, our current understanding of the factors controlling channel widening is still limited, as is our capability to predict it (Scorpio et al., 2018). Most of the studies analysed single river reaches affected by single flood events, and only a few of them extended the analysis to the catchment scale (e.g., Surian et al., 2016; Ruiz-Villanueva et al., 2018; Scorpio et al., 2018), but a larger-scale analysis (i.e., regional, multi-catchment scale), covering a large range of settings and several flood magnitudes, is still lacking. We aimed to fill this gap by compiling a large database with available information on channel widening after floods. We gathered a large spatial dataset from various mountain regions in Europe spanning different biogeographic settings (see Section 2.1) that allowed us to explore what type of floods produced larger widening and what typologies of rivers were more prone to widening.

We hypothesised that by compiling a large database we will be able to identify river reaches that respond differently to similar floods, in terms of channel widening. In addition, we expected that the meta-analysis will show and reinforce previous observations on the factors

controlling channel widening (i.e., valley confinement, artificial bank protections, and vegetated banks) and will make the first attempt to predict abrupt widening.

2. Material and methods

2.1. The channel widening database

An intensive compilation was done with data from previous studies, scientific publications, and technical reports, in which channel widening was analysed after individual floods. The data was collated using a standardized template containing selected variables for comparison and further analyses. An initial database contained information from 17 flood events that occurred in the last six decades (1957–2016) in various mountain regions (e.g., Northern Apennines, Carpathians, Alps, German Scarplands, Sardinia, and Pyrenees), across different European climate and geographic settings (i.e., Continental, Mediterranean and Alpine biogeographical regions; and Fig. 1), with a total of 85 rivers or streams, 94 segments (some rivers were analysed more than once in different segments affected by different floods) and 3330 river reaches.

Of the 3330 reaches gathered in the database, only reaches that experienced widening (i.e., showing width ratios >1) were considered in our meta-analysis ($n = 2850$). This assumption is further discussed in the discussion section. As not all records provided information for all relevant variables (e.g., discharge, drainage area), only those reaches with sufficient information (see following sections) were retained for the meta-analysis, resulting in a final dataset of 1564 river reaches (Table 2).

In the source references, the authors described the applied methods. In most cases, the methodology to gather the original data was based on the interpretation and mapping of high-resolution aerial or satellite imagery taken before and after the studied flood event. In some cases, field surveys were also carried out to verify the image-based results. Channel width before and after the floods and other morphological parameters were obtained using the remotely sensed data (see Section 2.2, and the source reference for further details). The authors used river reach as the study unit and divided the studied river segments into homogeneous reaches ranging from a few to hundreds of metres in length according to morphology (i.e., width, slope) or the presence of tributaries. Then different variables were extracted both at the river reach and at the catchment scale (see Section 2.2).

2.2. Data description

Each record in the database (i.e., river reach) was characterized by a river name, a reach ID, the corresponding country, biogeographical and climatic zones, flood date and peak discharge (Q_{max}). Detailed information on the floods (e.g., flood duration) or their triggering mechanisms (e.g., snowmelt) was not available in all cases. The reach morphological information provided by the source references included the initial and final channel width (i.e., channel width before (W_i) and after the flood event (W_{after}), the reach longitudinal slope (S), catchment area (A), and valley width (V_w). These parameters were obtained by the authors of the individual studies using aerial imagery, derived from digital elevation models, or observed in the field. We refer to the

Table 1
Review of selected central European studies focused on channel widening during single floods. The flood year, the return period estimated for the peak discharge as provided by the reference source, country, mountainous region, catchment area in km^2, and width ratio (W_r) are provided with the identified significant variables in the proposed equations to predict width ratio, the variance explained, and the source reference.

Flood date	Peak discharge return period (years)	Country	Region	Catchment area (km^2)	Width ratio	Significant variables	Proposed equation	Explained variance (%)	Reference
2005	~500	Austria	Alpine	172–1211	1.1–6.4	Spatial scale, flood unit stream power (*USP*) and mean unit stream power (*USPr*)	$W_r = 0.0007 \cdot USPr + 0.8182$ *(river reach scale)* $W_r = 0.2059 \cdot USP^{0.2949}$ *(local scale)*	72 31	Krapesch et al. (2011)
2011	>100	Italy	Northern Apennines	8.5–38.8	3.4–19.7	Flood unit stream power (*USP*), channel width before the flood (W_i)	$W_r = 0.07 * USP^{0.44}$ $W_r = 0.002 * USP$ $W_r = 25 W_i^{-1/2}$	44 upper envelopes	Comiti et al. (2016b)
2011	>100	Italy	Northern Apennines	8.5–38.8	3.4–19.7	Slope, flood unit stream power (*USP*), confinement index (*IC*), the percentage of reach length with artificial structures (*AS*), sediment supply (*SS*)	$W_r = -0.719 + 0.174 \cdot USP + 0.292 \cdot IC + 0.275 \cdot AS + 0.026 \cdot SS$ *(non-steep channels)* $W_r = -2.118 + 0.317 \cdot USP + 0.366 \cdot IC + 0.004 \cdot SS$ *(steep channels)*	38 67	Surian et al. (2016)
2013	>100	Italy	Sardinia	up to 685	1.1–6.2	Channel type, flood unit stream power (*USP*), confinement index (*IC*)			Righini et al. (2017)
2014	~150	Switzerland	Pre-alpine	0.2–93.7		Precipitation, slope, stream power index (*SPI*), forested channel length, sinuosity, and channel width before the flood (W_i)			Ruiz-Villanueva et al. (2018)
2015	100–150	Italy	Northern Apennines	5–307		Flood unit stream power (*USP*), confinement index (*IC*)	$W_r = 0.08 + 1.02 \cdot IC$ *(confined channels)* $W_r = 0.61 + 0.33 \cdot IC + 0.000033 USP$ *(unconfined channels)*	99 63	Scorpio et al. (2018)
2016	*triggering precipitation >100	Germany	South-western Germany	6–30	1.5–13.7	Flood unit stream power and flood stream power (*USP* and *SP*), confinement index (*IC*)	$W_r = 0.69 \cdot SP^{0.98}$ $W_r = 0.23 \cdot USP^{1.03}$ $W_r = 1.79 \cdot IC^{0.57}$ $W_r = -0.511 + 2.10 \cdot 10^{-4} \cdot USP + 0.208 \cdot IC$	73 66 64 67	Lucía et al. (2018)

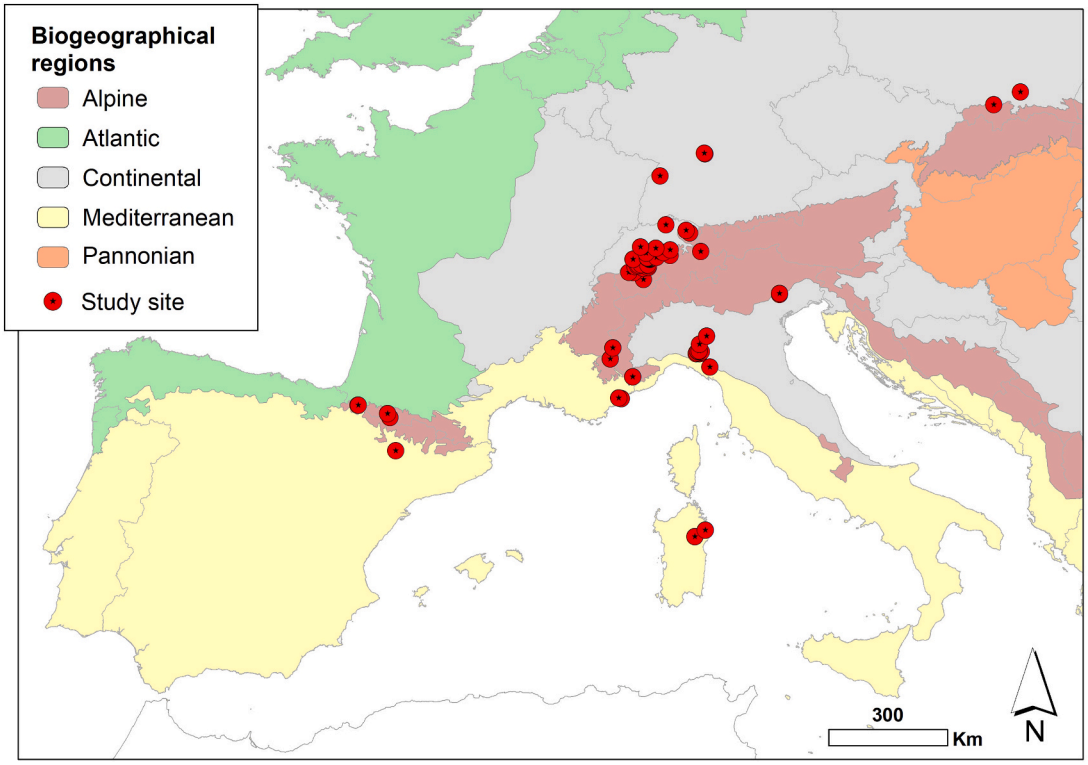

Fig. 1. Location of selected rivers (red dots) and the biogeographical regions (European Environmental Agency, 2016).

Table 2
Studies compiled for the meta-analysis that provided the 1564 selected reaches. The country where the studied site was located, number of streams or rivers, number of reaches, total reach length, reach slope, catchment area, channel width before the flood and the width ratio ranges and average values (in brackets) are provided.

Country	Number of rivers	Number of reaches	Total reach length, L [m]	Reach slope, S [m·m^{-1}]	Catchment area, A [km^2]	Channel width before the flood, W_i [m]	Width ratio, W_r [−]	References
France	8	965	160,155	0.002–0.20 (0.02)	7–945 (320)	5–250 (25)	1–14.40 (2.03)	Arnaud-Fassetta et al. (2005), Brousse et al. (2011), Felix De Almeida and Yassine (2018), Piton et al. (2018)
Germany	2	37	9086	0.01–0.15 (0.04)	0.9–30 (14)	2–8 (4)	1–13.76 (5.62)	Lucía et al. (2018)
Italy	7	166	68,530	0.001–0.21 (0.04)	0.1–303 (44)	3–77 (10)	1–19.68 (4.44)	Nardi and Rinaldi (2015), Surian et al. (2016), Amponsah (2017), Righini et al. (2017), Scorpio et al. (2018)
Poland	2	18	1800	0.001–0.02 (0.01)	17–599 (246)	11–118 (51)	1–5.17 (1.77)	Hajdukiewicz et al. (2016), Bednarska et al. (2018)
Spain	1	7	2100	0.024–0.11 (0.07)	241–251 (246)	16–48 (31)	1–5.43 (2.99)	Fernández Iglesias and Marquínez (2013), Marquínez et al. (2014)
Switzerland	31	371	69,728	0.007–0.36 (0.07)	1–346 (59)	1–130 (11)	1–4.44 (1.88)	Hunzinger and Durrer (2009), Bachmann (2012), Ruiz-Villanueva et al. (2018)

reference sources provided in Table 2 for further details.

Information derived for the purpose of this study, from the collected variables comprised the width ratio (W_r), (un)confinement index (*IC*: the ratio between valley width and channel width before the flood), specific peak discharge (*SQ;* peak discharge normalized by catchment area), total flood stream power ($SP = \rho \cdot g \cdot Q_{max} \cdot S$; where ρ is the flow density = 1000 kg·m^{-3}; g the gravitational acceleration 9.81 m·s^{-2}; Q_{max} is the flood peak discharge; and S is the longitudinal reach slope), and unit flood stream power (*USP*, i.e., the *SP* normalized by channel width) calculated using both the initial (*USP*) and final channel widths (USP_{after}). As the catchment area is correlated to several catchment characteristics (Anderson, 1957; Wohl and Merritt, 2008; Whitbread et al., 2015), to remove this potential catchment size effect from the analyses, we normalized the initial channel width (W_i*) and flood stream power (*SP**) by the catchment area applying a power coefficient equal to 0.44 as proposed by previous authors (Piégay et al., 2009; Alber and Piégay, 2017).

Table S1 in the supplementary material summarizes all variables included in the database.

The river reaches were additionally classified according to several categories to facilitate their description and make initial exploratory analyses:

i) we gathered data on the flood return period, and the triggering precipitation duration, and classified the events into three categories as follows: moderate floods <30, large floods between 30 and 100, and extreme floods >100 years return period; and short triggering precipitation event if duration <12 h, medium: 12–24 h, and long: >24 h duration.
ii) rivers were assigned to specific biogeographical (e.g., Mediterranean, Alpine, Continental; European Environmental Agency, 2016) and climatic regions (following the Köppen-Geiger climate classification; Rubel and Kottek, 2010), and were also classified according to their catchment areas (reaches with catchment areas (<10,10−100,100−300, >300 km^2) and in some cases, morphology and main lithology were also provided.
iii) reaches were grouped according to a channel width pre-flood class based on the frequency distributions shown in Fig. S1 (<10, 10–20, 20–50, >50 m), channel gradient class (<0.01, 0.01–0.04, 0.04–0.1 and > 0.1 m·m-1), confinement index class (≤2: confined: constrained by the valley bottom, which was still up to two times wider than the channel width before the flood; 2–4: partly confined; >4: unconfined: valley bottom up to four times larger than the channel width before the flood; Rapp and Abbe, 2003), percentage of forested channel length class (<50 and > 50 %), the presence of artificial lateral constraints or embankments (i.e., no constrained banks, one channelized bank, two channelized banks) before the flood, and in some cases, the main lithology.

Of the 1564 final selected reaches, most (69 %) were in the Alpine region, 23 % in the Mediterranean, and just 8 % in the Continental region. The dataset covered a large range of catchment areas (see Fig. S1 in the supplementary material), with 47 % of small basins (<100 km^2), 23 % of medium-sized basins (between 100 and 300 km^2), and 30 % of relatively large basins (>300 km^2). Most of the streams, 71 %, were relatively narrow streams (channel width before the flood <20 m), whereas wide rivers (with channel width before the flood >50 m) were only 7 % of the dataset. 76 % of the streams were flowing through gentle terrain, with slopes lower than 0.04 m m^{-1}, but there were also steep channels represented (18 % of reaches with slopes ranging between 0.04 and 0.1 m m^{-1}, and 6 % of very steep channels, with slopes >0.1 m m^{-1}). Just 18 % of the streams were classified as confined, 20 % as partially confined, and 62 % were unconfined channels.

In general, low-frequency, high-magnitude flood events over the last six decades were considered (59 % of reaches were affected by extreme floods >100 years return period), although more frequent floods were also included (19 % and 22 % of reaches were affected by large and moderate floods, respectively). Most of the floods included in our data occurred in summer (43 %) and autumn (48 %), while only a few occurred in winter (6 %) or spring (3 %). Moderate and large floods were generally triggered by longer precipitation and occurred in summer and autumn while extreme floods were mostly triggered by short precipitation events in the summer season.

Table 3 summarizes some of the most relevant variables of the 1564 reaches.

2.3. Data analysis

Statistical analyses were realized with the software RStudio (R Studio Team, 2018; R Core Team, 2021). To reduce the number of variables listed in Table S1 and described in the previous section, and to identify the main ones explaining most of the variability in our database, a multivariate factor analysis for mixed data was applied. The Factorial Analysis of Mixed Data (FAMD) generalizes a Principal Component Analysis (PCA) to datasets containing numerical and categorical variables. The goal of the FAMD was to transform the initial single variables into a set of linear combinations of these original variables called dimensions. The numerical variables were standardized (i.e., every variable had a mean value of zero and a unit variance value; Eager, 2017) before the FAMD analysis. The obtained dimensions from the FAMD, instead of single variables, were used to find major groups (i.e., clusters) within the 1564 river reaches by means of hierarchical clustering (*FactoMineR, Factoshiny,* and *factoextra* packages; Lê et al., 2008; Kassambara and Mundt, 2020; Vaissie and Husson, 2021). Details on this method are explained by Husson et al. (2010) and Kassambara (2017).

Differences within these major groups or between other classes or subsets (e.g., width ratio differences between clusters) were computed by the non-parametric Kruskal-Wallis test. We identified which pairs of groups were different by applying a post hoc pairwise comparison with Dunn's test (*Stats* package; R Core Team, 2021). Empirical cumulative distribution functions were computed for several groups (e.g., width ratio grouped by confinement class) to explore other variables not included in the FAMD (e.g., triggering precipitation duration) due to the limited data available, and the two-sample Kolmogorov-Smirnov test was applied to test differences between the distributions (*sfsmisc* package; Martin, 2021).

To predict the width ratio, we first extracted the relevant dimensions from the FAMD (those contributing with the largest percentage to the model; Fig. S2) and applied a multiple linear regression to them (FAMDR; *Stats* package; R Core Team, 2021); and second, we applied a Partial Least Squares Regression (PLSR; *pls* package; Mevik and Wehrens, 2007; Liland et al., 2022; Mevik and Wehrens, 2022) which basically employs a similar procedure. As we proved that the FAMDR and PLSR models performed in a similar way, we focused our analysis on FAMDR. We selected the variables that were contributing with the largest percentage to the dimensions of the FAMD and applied multiple regression to these variables as well. As they were not necessarily significant when used for predicting width ratio, we used stepwise regression to determine the final set of predictors. In addition, we computed bivariate regression using single variables (e.g., the confinement index or the stream power of the flood) as predictors. Both linear and non-linear models with one or multiple variables were explored to predict the width ratio using all data and the subsets from the identified clusters independently. Finally, we applied a non-linear quantile regression (Koenker and Park, 1994) to obtain upper envelopes (*quantreg* package; Koenker, 2022) by using all data. The quantile regression estimates the quantile value of a variable (e.g., W_r) with a specific non-exceedance probability *tau* (Koenker, 2005; Hao and Naiman, 2007); here, we used *tau* = 0.5 and 0.99. For all analyses, statistical significance was set to *p*-value <0.05.

Table 3
Minimum, 25th, 50th (median), 75th percentiles, maximum and standard deviation of drainage area, initial channel width, longitudinal slope, confinement index, specific discharge, and unit flood stream power for the 1564 selected reaches.

Variable	Min.	25th	Median	75th	Max.	St. Dev.
Drainage area [km^2]	0.05	13.39	130.24	411.48	944.71	252.59
Initial channel width [m]	1.30	7.10	13.21	22.50	250.00	25.41
Reach slope [m·m^{-1}]	0.001	0.01	0.02	0.04	0.36	0.04
Confinement index [−]	0.97	2.49	6.00	11.30	73.04	8.80
Specific peak discharge [$m^3 \cdot s^{-1} \cdot km^{-2}$]	0.17	0.83	1.18	8.99	59.40	7.04
Unit flood stream power [W·m^{-2}]	22.41	1281.93	2699.60	4565.68	48,062.64	5554.36

3. Results

3.1. Clustering the studied river reaches

Of 23 variables included in the database, 11 contained values for all selected reaches ($n = 1564$), and the FADM (Fig. 2a) identified eight as the most relevant (i.e., the biogeographical region, the return period class, reach slope, drainage area, confinement, specific or unit discharge, unit stream power, normalized stream power, and normalized initial channel width). The graph in Fig. 2a shows that variables related to the flow energy (i.e., slope, specific discharge, and stream power) contributed to the first dimension, while those related to the channel and valley geometry (i.e., confinement index and channel width) contributed to the second dimension. Still, the two first dimensions only explained 47 % of the variance (see also Fig. S2). These quantitative variables, and the categorical variables of biogeographical region and flood return period class, were used for establishing a typology of reaches in the cluster analysis.

Seven major groups (i.e., clusters) were identified in the hierarchical cluster according to the categorical and quantitative variables included in the dimensions of the FAMD (Fig. 2b). The 1564 reaches were grouped according to the seven clusters and their main characteristics were analysed and summarized here (and shown in Fig. 3).

The reaches grouped in Cluster 1 ($n = 380$) were located in the Alpine region (98 %), affected by moderate floods (82 %), unconfined (62 %), partly confined (24 %), and confined (14 %) channels, between 10 and 50 m wide (85 %) and with a moderate low to low slope (98 %). The 241 reaches grouped in Cluster 2 were also located in the Alpine region, entirely affected by large floods, unconfined channels (96 %), relatively narrow (78 % with an initial channel width lower than 20 m), with moderate slopes ranging between 0.04 and 0.1 $m \cdot m^{-1}$ (88 %). Cluster 3 ($n = 69$) had Alpine (88 %) reaches affected by extreme (77 %) and moderate (23 %) floods, located in confined (43 %) and partly confined (41 %) channels, relatively wide (initial width ranging between 20 and 50 m for 41 % and larger than 50 m for 55 %), and of moderate low (62 %) to low slope (26 %). Cluster 4 ($n = 412$) grouped Alpine reaches (98 %), entirely affected by extreme floods, mostly unconfined (70 %), relatively narrow channels (45 % <20 m wide, and 35 % <10 m wide), and relatively steep (slopes ranging between 0.04 and 0.1 $m \cdot m^{-1}$ for 72 %), and very steep (20 %) slopes (>0.1 $m \cdot m^{-1}$).

The smallest cluster was Cluster 5, with 84 river reaches located in the Continental region (100 %), affected mainly by extreme (56 %) and large (30 %) floods, in partly confined (25 %) and unconfined channels (67 %), of <20 m initial channel width (81 %) and moderate slope (70 % lower than 0.04 m m^{-1}).

Two clusters grouped Mediterranean reaches. Cluster 6 ($n = 235$), was characterized by Mediterranean reaches only, affected by extreme (87 %) and large (13 %) floods, located in confined (60 %), partly confined (23 %), and unconfined (17 %) channels, with narrow channels (92 % <20 m wide) and low slopes (91 % <0.01 $m \cdot m^{-1}$). While Cluster 7 ($n = 143$) had mostly Mediterranean reaches (73 %), mixed with a few Continental (27 %) reaches, all affected by extreme floods (99 %), with unconfined (82 %), narrow (84 % with channel width < 10 m), and moderate (59 %) to a relatively high (39 %) slope.

Table 4 summarizes the main variables for each cluster.

Fig. 4 shows some illustrative reaches from each cluster before and after flood events.

3.2. Contrasting response to floods in terms of widening among the seven clusters

The channel width before and after the flood, the total widening, and the width ratio (W_r) within the clusters significantly differed (p-value Kruskal Wallis <0.001; Fig. 5).

Table 5 summarizes the main statistics for the widening-related variables (i.e., channel width before and after, total widening, and

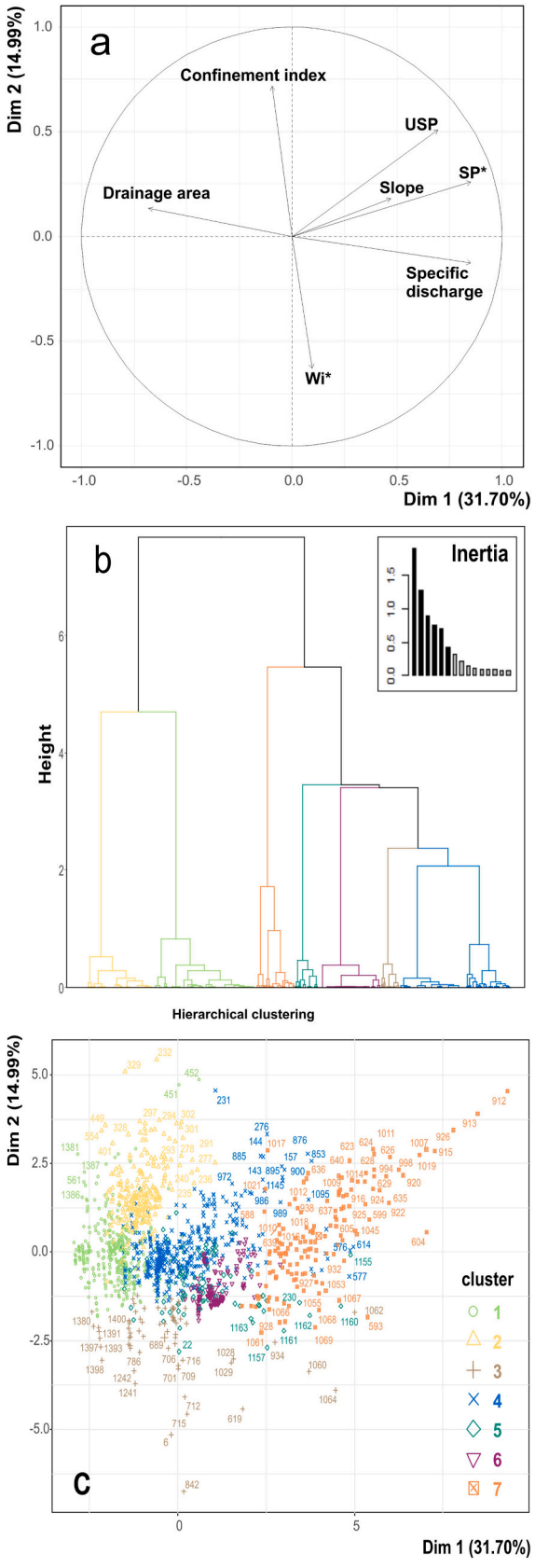

Fig. 2. (a) FAMD correlation circle of quantitative variables; (b) hierarchical clustering dendrogram showing the seven clusters obtained based on the FAMD dimensions; the small plot shows the inertia and number of clusters; (c) factor map coloured by clusters showing the reaches ID. USP: unit stream (flood) power; SP*: normalized stream power; *Wi**: normalized initial channel width.

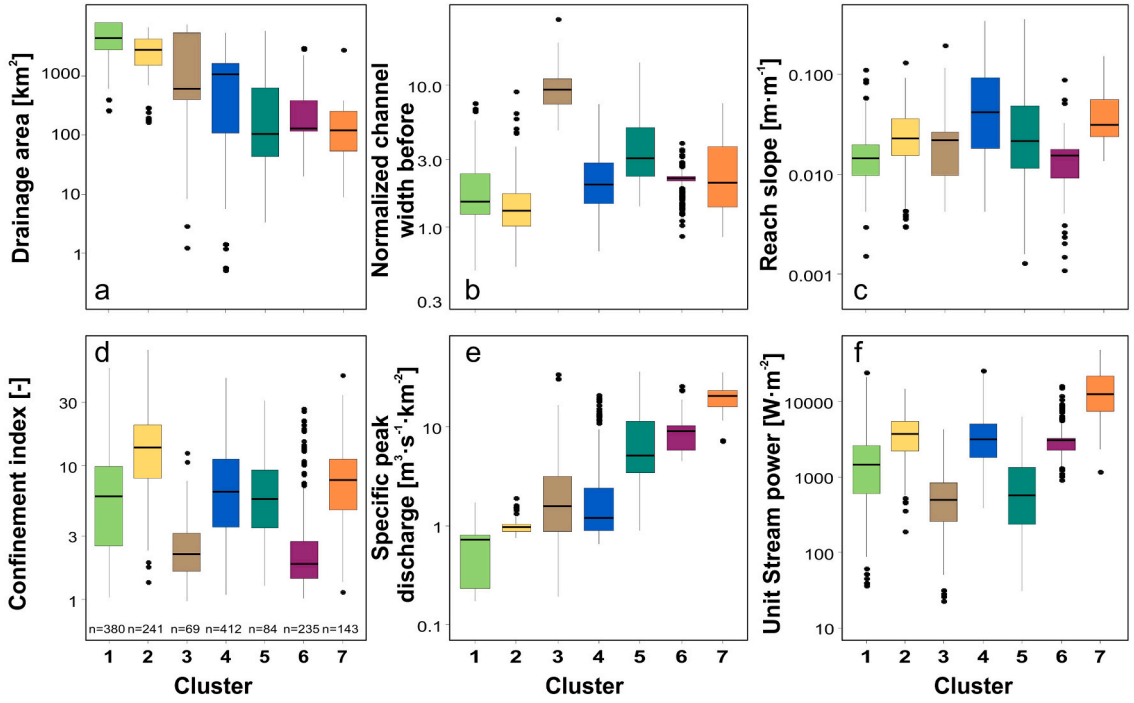

Fig. 3. Boxplots of drainage area, normalized channel width before the flood, reach longitudinal slope, confinement index, specific peak discharge, and unit stream power (flood power) by cluster. n = sample size. The boxes' bottom and top indicate the first and third quartiles, respectively; the line inside the boxes is the median, and the dots are outliers.

width ratio).

The most significant width ratio was observed for clusters 7, 6, and 4 (mean values were 5, 2.3, and 2.5, respectively). However, in terms of total widening (difference between the pre- and post- flood channel width in meters), cluster 3 showed the largest value (mean = 39 m, median = 30 m). Reaches of cluster 3 were the widest before the floods (mean initial channel width = 86 m), and thus width ratio was generally low (mean = 1.7). Clusters 4 and 7 also showed large total widening values (mean = 22 m and 26 m, median = 10 m, and 23 m respectively). The reach experiencing the largest total widening (235 m) was grouped in cluster 1 (Table 5).

We observed that clusters 7 and 4, which showed the largest widening, also were those with the steepest reaches (Table 4; Fig. 3c). When looking at the reaches characterized by the different slope classes within clusters, we observed, however, small differences. In general, channels with intermediate slope (i.e., the gradient between 0.01 and 0.1 m ·m^{-1}) widened slightly more than steeper reaches (gradient >0.1 m ·m^{-1}) or reaches with a very gentle slope (gradient <0.01 m ·m^{-1}). But differences were, in general, not significant. Very few reaches were classified according to their morphological channel pattern (i.e., meandering-wandering, braided, or straight; n = 342). For all reaches together, we did not find significant differences in width ratio for reaches with different channel patterns. Still, some clusters showed some differences. Single-thread channels of clusters 1 and 3 widened more than multi-thread ones, whereas the opposite was observed in the reaches of cluster 4. The latter is one of the clusters showing the largest width ratio values in the dataset. Unfortunately, the reaches of clusters 2, 5, and 7 did not provide information about the morphology.

River reaches located in different regions behaved differently regarding channel widening, with those located in the Mediterranean region showing a significantly larger widening (clusters 6 and 7) than the reaches in the other regions. However, the region where the reach was located was not the only factor explaining the width ratio. Four of the seven clusters grouped reaches located in the Alpine region (i.e., Clusters 1, 2, 3 and 4), as this is the region with the largest number of reaches in the database. Comparing the four clusters with Alpine reaches, we could see that reaches of cluster 4 widened significantly more than reaches of the other three Alpine clusters. All reaches of cluster 4 were affected by extreme floods, as were most in cluster 3. Reaches of cluster 4 were mainly unconfined (mean IC = 8.4), relatively narrow (mean initial channel width = 13.6 m), and relatively steep channels (mean gradient = 0.06 m·m^{-1}), while reaches of cluster 3 were confined and partly confined (mean IC = 2.7), relatively wide (mean initial channel width = 86 m), and of moderate low slope channels (mean gradient = 0.02 m·m^{-1}). Therefore, the flood magnitude mattered but was not the only factor controlling the river response in terms of widening; channel and valley morphology also played a role, as well as other variables.

3.3. The role of moderate floods and the triggering precipitation

In general, extreme floods caused a larger widening in all reaches when analysed together and in the reaches of cluster 1 (Fig. 6a,c), but some clusters showed some exceptions. We observed that the reaches of clusters 5 and 6 affected by moderate, large, and extreme floods experienced similar widening in all cases (Fig. 6b,d). Even a few reaches of cluster 5 (Continental reaches) experienced larger widening after large floods than after extreme floods. However, the number of reaches was very low. The width ratio was not different between the Alpine reaches in cluster 6 affected by extreme and large floods. Reaches of clusters 2, 3, 4 and 7 were affected mostly or entirely by one flood frequency class and thus could not be used for the comparison.

The analysis of the flood-triggering precipitation duration (for those reaches for which we had such information) revealed significant differences between the groups. In general, floods triggered by shorter precipitation events (e.g., flash floods) caused larger widening than floods triggered by longer precipitation events, as shown in Fig. 7 for all reaches and reaches of cluster 6 (i.e., Mediterranean reaches, confined and partly confined narrow and low slope). However, for reaches of cluster 4 (i.e., Alpine reaches affected by extreme floods, unconfined, relatively narrow, and steep channels), floods with longer precipitation duration produced significantly larger widening than those triggered by

Table 4
Minimum, 25th, 50th (median), 75th percentiles, mean, and maximum of drainage area, normalized channel width, longitudinal slope, confinement index, specific discharge, and unit flood stream power for the 1564 selected reaches grouped by clusters.

Cluster	Min.	25th	Median	Mean	75th	Max.
Drainage area [km^2]						
1	26.0	281.1	450.0	499.8	805.1	944.7
2	16.4	156.3	279.0	288.3	436.3	681.9
3	0.1	41.0	62.0	223.5	551.4	750.5
4	0.1	11.1	108.1	125.8	165.8	551.4
5	0.3	4.3	10.5	70.8	63.6	599.3
6	2.0	11.7	13.1	40.5	38.7	302.9
7	0.9	5.4	12.1	16.8	25.6	284.0
Normalized channel width before flood [−]						
1	0.5	1.2	1.5	2.0	2.4	7.5
2	0.5	1.0	1.3	1.5	1.7	9.0
3	4.8	7.4	9.3	9.9	11.2	29.5
4	0.7	1.5	2.0	2.3	2.8	7.4
5	1.4	2.3	3.0	4.0	5.1	14.6
6	0.9	2.1	2.2	2.1	2.3	3.9
7	0.8	1.4	2.1	2.6	3.7	7.4
Longitudinal slope [m·m^{-1}]						
1	0.002	0.010	0.014	0.017	0.020	0.110
2	0.003	0.015	0.023	0.028	0.036	0.132
3	0.004	0.010	0.022	0.026	0.026	0.195
4	0.004	0.018	0.042	0.062	0.091	0.340
5	0.001	0.011	0.022	0.045	0.048	0.357
6	0.001	0.009	0.016	0.015	0.018	0.087
7	0.013	0.024	0.031	0.042	0.056	0.151
Confinement index [−]						
1	1.0	2.5	5.9	8.7	9.9	53.9
2	1.4	8.1	13.7	16.1	20.1	73.0
3	1.0	1.6	2.2	2.8	3.1	12.5
4	1.1	3.5	6.4	8.4	11.2	45.5
5	1.3	3.5	5.7	7.4	9.3	30.9
6	1.0	1.4	1.8	3.6	2.7	26.6
7	1.1	4.7	7.8	9.0	11.2	47.5
Specific peak discharge [m^3·s^{-1}·km^{-2}]						
1	0.17	0.23	0.72	0.67	0.81	1.72
2	0.76	0.88	0.96	1.00	1.03	1.91
3	0.19	0.87	1.57	3.78	3.15	33.89
4	0.66	0.89	1.19	3.22	2.42	21.08
5	0.90	3.41	5.16	9.31	11.39	35.83
6	4.51	5.84	9.01	8.95	10.17	25.54
7	7.22	15.83	20.40	20.73	23.41	59.40
Unit flood stream power [W·m^{-2}]						
1	35.8	595.0	1439.3	1962.1	2594.2	24,306.7
2	188.8	2220.8	3718.7	4274.2	5510.6	14,781.0
3	22.4	252.5	495.0	607.7	837.1	4282.5
4	391.5	1792.2	3171.1	4185.7	5040.3	25,998.3
5	30.5	236.2	576.0	1091.7	1352.2	6340.7
6	901.0	2295.0	3061.0	3258.0	3283.0	15,962.0
7	1162.0	7514.0	12,576.0	15,595.0	21,570.0	48,063.0

medium and short rainfall. Short precipitation was responsible for the floods affecting all reaches of cluster 7 (i.e., Mediterranean reaches affected by extreme floods, with unconfined, narrow, and steep channels), whereas long precipitation duration triggered the floods, causing the widening in all reaches of clusters 1, and 2 (Alpine reaches affected by moderate and large floods). The width ratio value did not show any significant difference between reaches affected by floods triggered by precipitations of different durations in clusters 5 and 3.

3.4. The role of vegetation and bank reinforcement

A subset of reaches contained information about the percentage of forested channel length (n = 777), with a majority of reaches being densely forested (mean percentage of forested channel length = 85 %). In general, and for all reaches together, we observed lower values of width ratio in rivers with >50 % of forested banks than for river reaches with a lower percentage of forested banks. This was also true for reaches grouped in cluster 1 (Fig. 8). Densely and sparsely forested reaches of clusters 3, 4, and 5 did not show significant differences in terms of width ratio. The reaches characterized by the largest width ratios (i.e., 6 and 7) did not have enough information to make a comparison and explore the effect of vegetation, being most reaches of cluster 6 densely forested. No information was available for most reaches of cluster 7.

From those reaches that contained information about the artificial reinforcement or protection of riverbanks (i.e., channelization) in the database (n = 991), most reaches (74 %) had no protection, 21 % had one artificially reinforced bank, and only 4 % had two reinforced banks. In general, we observed that reaches with no reinforcement or only one reinforced bank widened more than reaches with two reinforced banks. More interestingly, reaches with one reinforced bank showed significantly higher width ratios than reaches with no reinforcement for all reaches together and for reaches in cluster 1. However, due to the low number of reaches with this information and the inequity in the number of reaches with and without reinforced banks, results were limited to making a robust comparison between clusters.

3.5. Towards the prediction of channel widening

We selected the two first dimensions from the FAMD (see Fig. S2) and applied a linear regression to them, and we applied the PLSR with the first three components that were shown to be relevant (Fig. S3). The results proved that these two multivariate models fitting all data had a very low prediction capability ($R^2 < 0.2$). The two dimensions from the FAMD and the three components from the PLSR explained only 17 % and 18 % of the variance when used for the prediction of the width ratio, respectively. For simplicity, we focused on the regression of FAMD dimensions only. The FAMDR performance in terms of residuals is shown in Fig. S4.

The quantitative variables that contributed more to the FAMD dimensions 1 and 2 were the specific peak discharge (SQ), the normalized stream power (SP^*), the unit stream power (USP), the confinement index (IC), and the normalized initial channel width (W_i^*), and in a lower percentage the drainage area (A) and the reach slope (S; Fig. S2). The stepwise regression of these variables showed that the significant predictors of the width ratio were the specific peak discharge (SQ), the unit stream power (USP), and the reach slope (S). The drainage area (A), the confinement index (IC), and the normalized initial channel width (W_i^*) were not found significant predictors. Still, following what has been done in previous works, we decided to explore models including the confinement index as well. The prediction capability of the 2 main obtained models (here referred to as model 1 and model 2) for all data was very low ($R^2 < 0.3$).

The obtained bi- and multi-variate models are reported here, in Table 6 and in Fig. S4:

Model 1: $W_r \sim 1.90 + (4.6e\text{-}05 \cdot SP^* + 6.8e\text{-}02 \cdot SQ + 8.2e\text{-}03 \cdot IC - 1.3e\text{-}01 \cdot W_i^*)$

Residual standard error: 1.65; Multiple R^2: 0.21

Model 2: $W_r \sim 1.75 + (-9.22 \cdot S + 1.370e\text{-}04 \cdot USP + 6.305e\text{-}02 \cdot SQ)$

Residual standard error: 1.57; Multiple R^2: 0.28

We compared the reported width ratio values with the predicted ones using the multivariate models PLSR, FAMDR, Models 1 and 2, and Eqs. 17 and 18 reported in Table 3 (Fig. 9). The comparison showed that the models performed very similarly when using all data, showing a strong underestimation of large width ratios in all cases. The PLSR model,

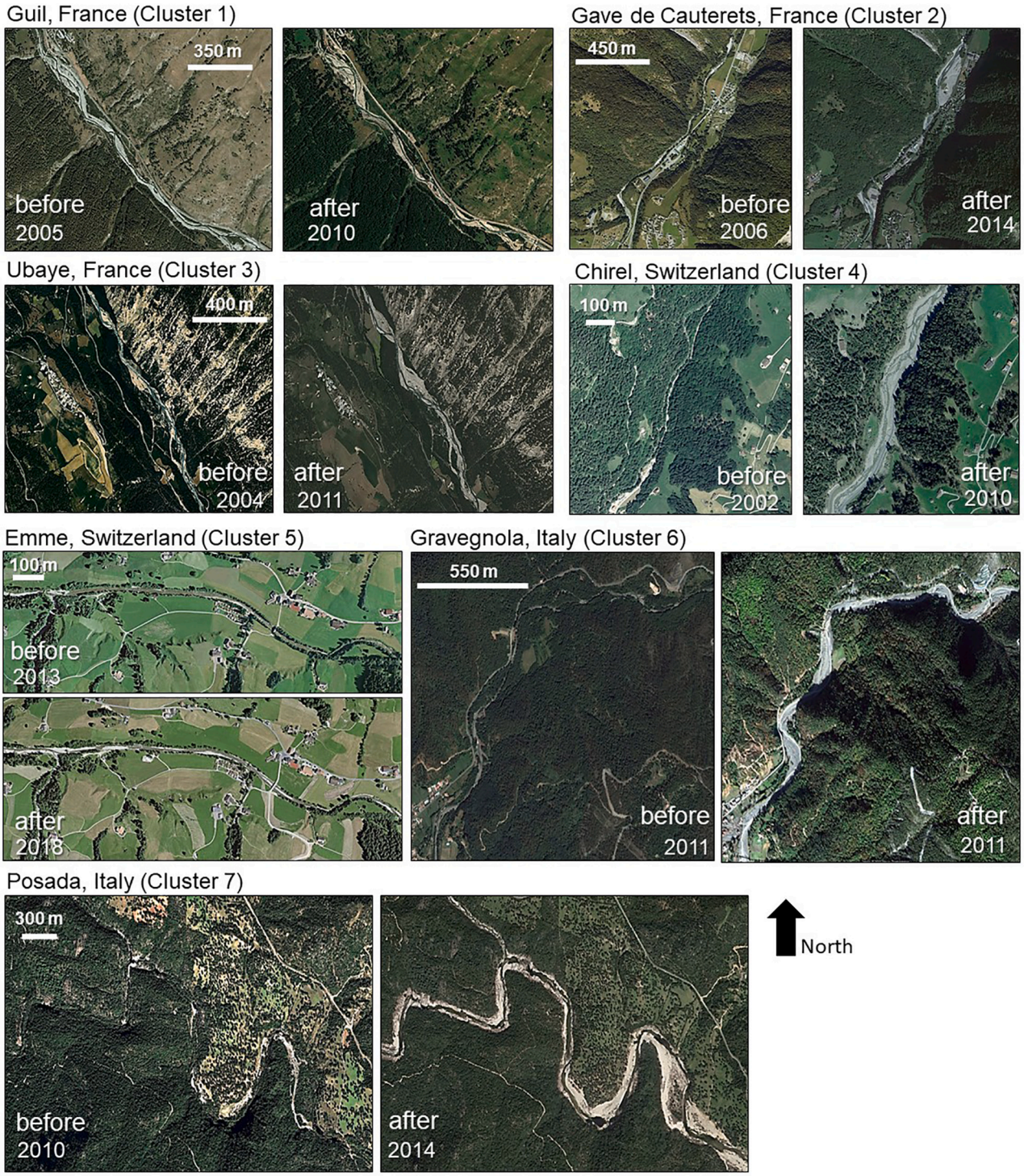

Fig. 4. High-resolution satellite and aerial images from ©Google Earth of some selected reaches from the seven clusters before and after a flood event (and the years). All images are oriented pointing North on top, the scale is shown in all images from before the flood.

model 2 ($W_r \sim S + USP + SQ$), and eq. 18 ($W_r \sim USP + IC$) showed slightly better performance for all data in terms of MAE, MSE, and RMSE (Fig. 9).

The models were also fitted to the seven clusters independently and their prediction capability varied significantly (Fig. 10). The R^2 of Model 1 ($W_r \sim 1.90 + 4.6e\text{-}05 \cdot SP^* + 6.8e\text{-}02 \cdot UQ + 8.2e\text{-}03 \cdot IC - 1.3e\text{-}01 \cdot W_i^*$) ranged between 0.002 and 0.42, with the largest values obtained for cluster 7 ($R^2 = 0.42$), cluster 6 ($R^2 = 0.42$), and cluster 1 ($R^2 = 0.24$). Similarly, the R^2 of Model 2 and eq. 18 ($Wr \sim USP + IC$) showed large R^2 values for clusters 7 ($R^2 = 0.35$ and 0.46), and 6 ($R^2 = 0.29$ and 0.36). As model 1 showed generally larger R^2 values, we showed the comparison with observed values in Fig. 10.

The upper envelopes (99 % regression quantile) obtained from the quantile regression (see Fig. S5 showing the fitting lines to individual variables), provided a good fit for the largest values of observed width ratio for all data, and may represent a good prediction of worst-case scenarios and upper boundaries (Fig. 11).

The evaluation of the performance for predicting the width ratio (in

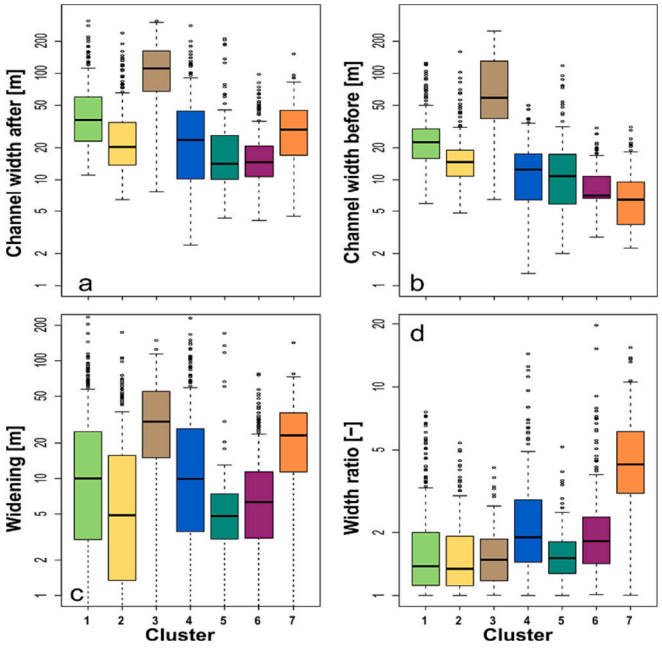

Fig. 5. Boxplots of channel width after (a) and before (b) the flood, total widening (c; i.e., the difference between channel width before and after), and width ratio (d) for the seven clusters.

Table 5
Minimum, 25th, 50th (median), 75th percentiles, mean, and maximum of channel width after and before the flood, total widening, and width ratio for the 1564 selected reaches grouped by clusters.

Cluster	Min.	25th	Median	Mean	75th	Max.
Channel width after flood						
1	11.1	23.1	36.5	49.8	60.0	310.0
2	6.4	13.8	20.3	32.5	34.5	238.7
3	7.7	67.7	110.9	125.0	162.4	310.0
4	2.4	10.2	23.7	35.1	44.1	280.0
5	4.3	10.1	14.1	30.3	26.1	212.0
6	4.1	10.7	14.6	19.1	20.8	97.7
7	4.5	17.0	29.6	34.0	45.0	152.3
Channel width before flood						
1	5.9	15.9	22.6	29.0	30.0	125.0
2	4.8	10.8	14.7	18.3	19.0	159.4
3	6.4	37.5	58.9	86.3	130.0	250.0
4	1.3	6.4	12.5	13.6	17.5	50.0
5	2.0	5.9	10.8	18.4	17.3	118.0
6	2.8	6.6	7.0	8.8	10.8	30.6
7	2.3	3.7	6.4	7.7	9.6	31.3
Total widening						
1	0.04	3.01	10.00	20.83	25.00	235.00
2	0.00	1.34	4.89	14.22	15.70	174.31
3	0.48	15.00	30.40	38.70	55.00	149.00
4	0.40	3.50	9.95	21.52	26.50	230.00
5	0.09	3.01	4.80	11.97	7.44	171.00
6	0.10	3.07	6.30	10.35	11.40	77.51
7	0.02	11.37	23.27	26.27	36.15	142.40
Width Ratio						
1	1.0	1.1	1.4	1.9	2.0	7.6
2	1.0	1.1	1.3	1.7	1.9	5.4
3	1.0	1.2	1.5	1.7	1.9	4.1
4	1.0	1.4	1.9	2.5	2.9	14.4
5	1.0	1.3	1.5	1.7	1.8	5.2
6	1.0	1.4	1.8	2.3	2.4	19.7
7	1.0	3.1	4.3	5.0	6.1	15.4

terms of mean absolute, standard, and root squared errors) of the upper envelopes presented in Table 6 revealed that eqs. 12, 14, and 15 performed slightly better than the others (Fig. 11), with *USP*, *SP** and *IC* as predictors.

4. Discussion

4.1. Limitations

The large dataset compiled for this work allowed us to characterize river reaches prone to large widening and to propose empirical equations to predict large channel widening during floods at the reach scale. Still, some limitations should be discussed.

First, we acknowledge that the representativeness of our database is limited to certain regions, river types and conditions (i.e., those represented in the seven clusters) but would not cover the full range of natural variability of geomorphic responses in European rivers or elsewhere. The heterogeneity of natural systems, such as rivers, is linked to their high spatial and temporal variability controlled by many environmental factors not represented in our database.

Second, the database analysed in the present work is composed of data gathered after flood events that triggered significant geomorphic changes, including channel widening. Consequently, the database is affected by a bias as it only includes sites that experienced channel widening. As stressed by Ruiz-Villanueva et al. (2018), the inclusion of reaches which did not widen may reveal that reaches with similar characteristics exhibit significantly different responses during the same flood event.

Third, there are important limitations regarding the availability of data. For example, only some reaches included in our database had information about the peak discharge of the flood, and very few had more details, such as the flood hydrograph (Amponsah et al., 2016). Therefore, we classified the events by the return period classes and the triggering precipitation duration. However, the flood duration is a key variable, as a flood that exceeds a certain threshold discharge (i.e., related to certain energy or unit stream power, for example), 300 $W \cdot m^{-2}$ according to Buraas et al. (2014), for a very short time might result in smaller widening than a longer flood of the same magnitude (Rhoads, 2020). Thus, this information should be, when possible, included in the analyses. Additional hydraulic variables, such as the Froude number, could also provide more insights into the flow energy and its control on channel adjustments (Piton and Recking, 2019). The flood history matters as well (Beven, 1981; Brunsden, 2001; Ockelford et al., 2019); after a long period without a major flood, channels may experience narrowing (Liébault and Piégay, 2002; Liébault et al., 2005), but they might widen again if a flood with sufficient energy occurs (Arnaud-Fassetta et al., 2005). On the other hand, the occurrence of a second large flood in a relatively short time may not produce any significant morphological change (Rhoads, 2020).

Climate plays an important role in determining the flood regime and, thus, the river response and channel width (Wolman and Gerson, 1978; Fryirs et al., 2015; Feng et al., 2022). We included only partially this information, as the dataset did not cover a wide range of different climate regions to make robust comparisons. New developed open data sources that provide insights into the hydrological regime and variability at the European level could be explored (e.g., Kuentz et al., 2017); however, the spatial scale remains too coarse for our study.

Reaches characterized by different channel planforms, morphologies, and underlaid lithologies respond differently to floods (e.g., Fratkin et al., 2020); however, the available information was limited, and the observed patterns were not ubiquitous.

Besides the current channel morphology, to understand the response to floods, we should also consider the past evolution or river trajectory over the last century and human influence (Belletti et al., 2014; Hohensinner et al., 2021; Scorpio and Piégay, 2021). Each river follows a complex trajectory of morphological changes where long-term trends

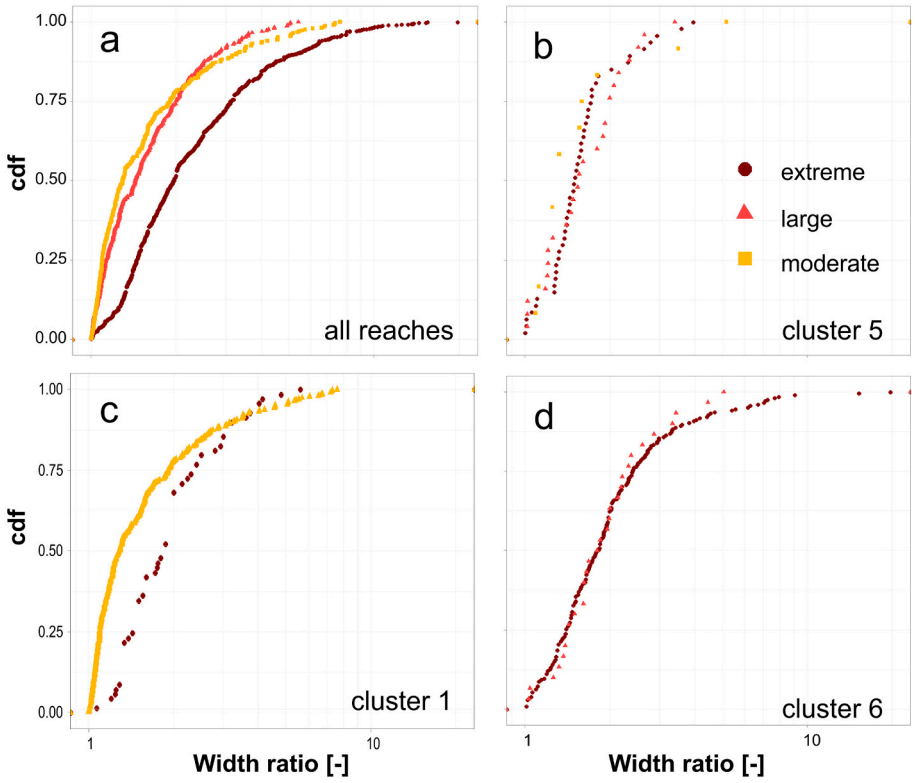

Fig. 6. Cumulative distribution functions (cdf) of width ratio for all reaches grouped by flood return period class (i.e., extreme: return period >100 years; large: >30 return period ≤100; moderate floods: <30 years) and clusters 1, 5 and 6.

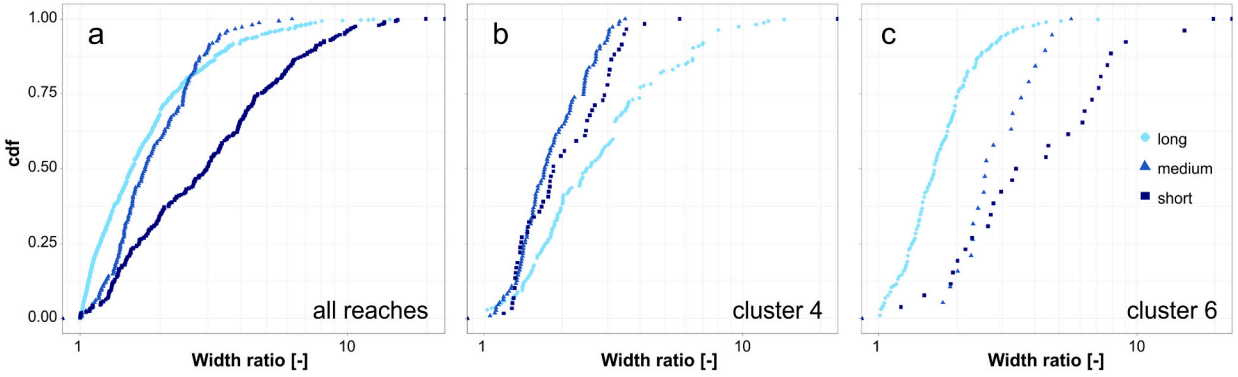

Fig. 7. Cumulative distribution functions (cdf) of width ratio for all reaches grouped by flood triggering precipitation duration class (i.e., <12 h: short, 12–24 h: medium, >24 h: long duration) and clusters 4 and 6.

and short-term disturbances overlap (Brierley et al., 2008; Dufour and Piégay, 2009; Nardi and Rinaldi, 2015). Thus, we can argue that probably some narrow channels could have been wider or even braided channels some time ago, and the response to flood is going back to the natural range of variability (Segura-Beltrán and Sanchis-Ibor, 2013; Dean and Schmidt, 2013; Wyżga et al., 2016; Hohensinner et al., 2021). Our dataset did not allow us to develop this aspect further, but we could expect that a river that underwent notable narrowing in the past could be more prone to widen than others.

Channel width is known to be related to the presence of vegetation (Hey and Thorne, 1986), and the effect of vegetation on bank erosion is widely recognised (Abernethy and Rutherfurd, 2001; Pollen et al., 2004; Vargas-Luna et al., 2019). The type (i.e., size, species, and root reinforcement) and density of the vegetation might be also important aspects to take into account (Hickin, 1984; Pollen, 2007; Perignon et al., 2013). However, we only analysed the percentage of the channel length covered by vegetation.

In addition to vegetation, channel-bed and -bank grain size is a major variable that controls sediment entrainment and, thus bed and bank erosion (Shields, 1936). However, only limited data were available in our database (e.g., Bachmann, 2012). Still, the relationship between the presence of vegetation and the channel sediment grain size deserves more attention (Török and Parker, 2022).

Not just grain size and its relation to incipient motion controls channel changes, but sediment supply may play a role, too (Pfeiffer et al., 2017). River reaches fed by large amounts of coarse sediment may be characterized by unstable, aggrading, and wide channels, while reaches with limited sediment supply, for example regulated by dams, may incise and become narrower (Williams and Wolman, 1984; Harvey, 1991; Wohl et al., 2015). The identification of sediment sources, their connectivity to the channel, and the supply of sediment were rarely assessed in the compiled studies (e.g., Surian et al., 2016; Scorpio et al.,

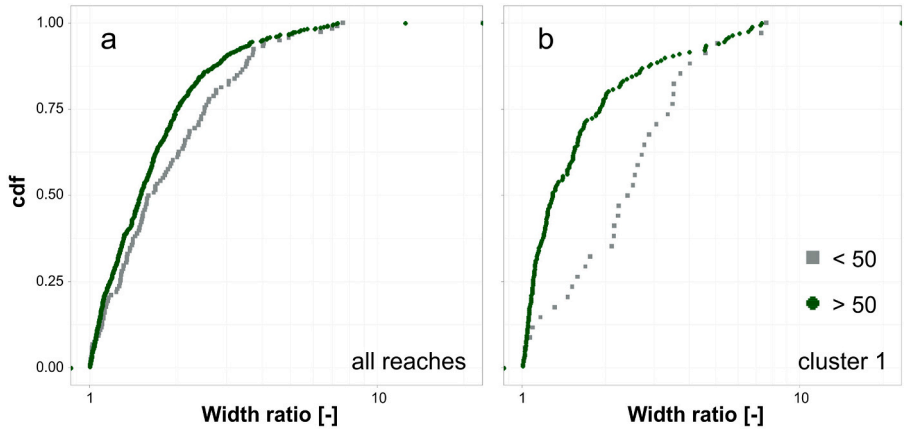

Fig. 8. Cumulative distribution functions (cdf) of width ratio for all reaches grouped by forested channel length class (> or < 50 %) and cluster 1.

Table 6
Multi- and bi-variate linear and non-linear equations obtained by the quantile regression and upper envelopes (see Figs. 9, 10 and 11).

Explanatory variables used in the equations to predict W_r	Equations obtained by the quantile regression (0.5)	Upper envelope equations (quantile 0.99)
Initial channel width (W_i)	[Eq.1] $W_r \sim 2 \cdot W_i^{0.13}$ $W_{after} \sim 2 \cdot W_i^{-0.1}$	[Eq.6] $W_r \sim 20 \cdot W_i^{-0.33}$
Normalized initial channel width (W_i *)	[Eq.2] $W_r \sim 2 \cdot W_i{*}^{-0.1}$	[Eq.7] $W_r \sim 13 \cdot W_i{*}^{-0.4}$
Confinement index (IC)	No Significant	[Eq.8] $W_r \sim 3 \cdot IC^{0.5}$
Stream flood Power (SP)	[Eq.3] $W_r \sim 6 \cdot 10^{-6} \cdot SP$	[Eq.9] $W_r \sim 6 \cdot 10^{-5} \cdot SP$ [Eq.10] $W_r \sim 0.3 \cdot SP^{0.32}$
Unit Stream flood Power (USP)	[Eq.4] $W_r \sim 0.0001 \cdot USP$	[Eq.11] $W_r \sim 0.0004 \cdot USP$ [Eq.12] $W_r \sim 0.5 \cdot USP^{0.32}$
Normalized stream flood Power (SP*) and Confinement index (IC)	[Eq.5] $W_r \sim 7 \cdot 10^{-5} \cdot SP{*}$ $W_r \sim 1.6 + 0.0001 \cdot SP{*} + 0.0012 \cdot IC$	[Eq.13] $W_r \sim 0.0002 \cdot SP{*}$ [Eq.14] $W_r \sim 0.9 \cdot SP{*}^{0.25}$
Unit Stream flood Power (USP) and Confinement index (IC)	[Eq.18] $W_r \sim 1.7 + 0.00016 \cdot USP + 0.0012 \cdot IC$	[Eq.15] $W_r \sim IC^{0.8} + USP^{0.1}$
Stream (flood) Power (SP) and Confinement index (IC)	Not Significant	[Eq.16] $W_r \sim IC^{0.8} + SP^{0.1}$

2022). Interestingly, some studies showed that sediment supply was not the relevant driver for channel widening (Milan, 2012; Surian et al., 2016; Scorpio et al., 2018), contrastingly to other works that observed sediment supply as a major driver of channel changes (Harvey, 2001; Bertrand and Liébault, 2019; Surian et al., 2020; Brenna et al., 2023). Therefore, further research is still needed to better understand the role of sediment supply in the geomorphic response to floods.

Despite these limitations, our results shed light on understanding complex river responses to floods and their drivers.

4.2. Variables driving abrupt widening

Our results showed that, in general, extreme floods, triggered by relatively short and intense precipitation events, were responsible for larger widening, particularly in the Mediterranean region (cluster 7). This is not a surprising result (e.g., Gaume et al., 2016), still, it is of utmost importance regarding flood management in the Mediterranean region. The role of smaller floods (i.e., large, and moderate events) was also revealed by our results. Some reaches of clusters 1, 2, 3, and 5 affected by moderate and large floods widened up to 7 times their initial

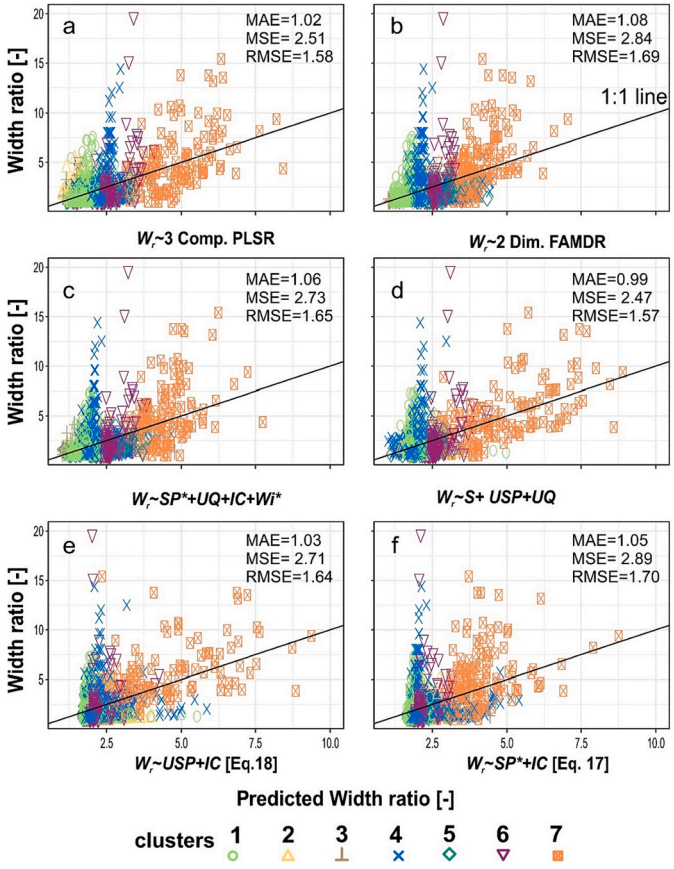

Fig. 9. Observed width ratio (W_r) versus predicted values obtained by applying the models described in the text and shown in Table 6, for all data coloured by clusters. The black line is the 1:1 line: (a) 3 Comp. PLSR: three first components from PLSR; (b) 2 Dim. FAMDR: two first dimensions from FAMD; W_i: initial channel width; W_i*: normalized initial width; IC: confinement index; SQ: specific peak discharge; USP: unit flood stream power; SP: stream (flood) power; SP*: normalized stream power. MAE: mean absolute error; MSE: mean standard error; RMSE: root mean squared error.

channel width. Reaches of clusters 5 and 6 did not show significant differences in width ratio for reaches affected by floods with different return periods (Fig. 6), probably also explained by the high degree of confinement, particularly of cluster 6 (Fig. 3).

Therefore, it is not just the magnitude but also other variables, for example, the duration of the flood, that determine the geomorphic

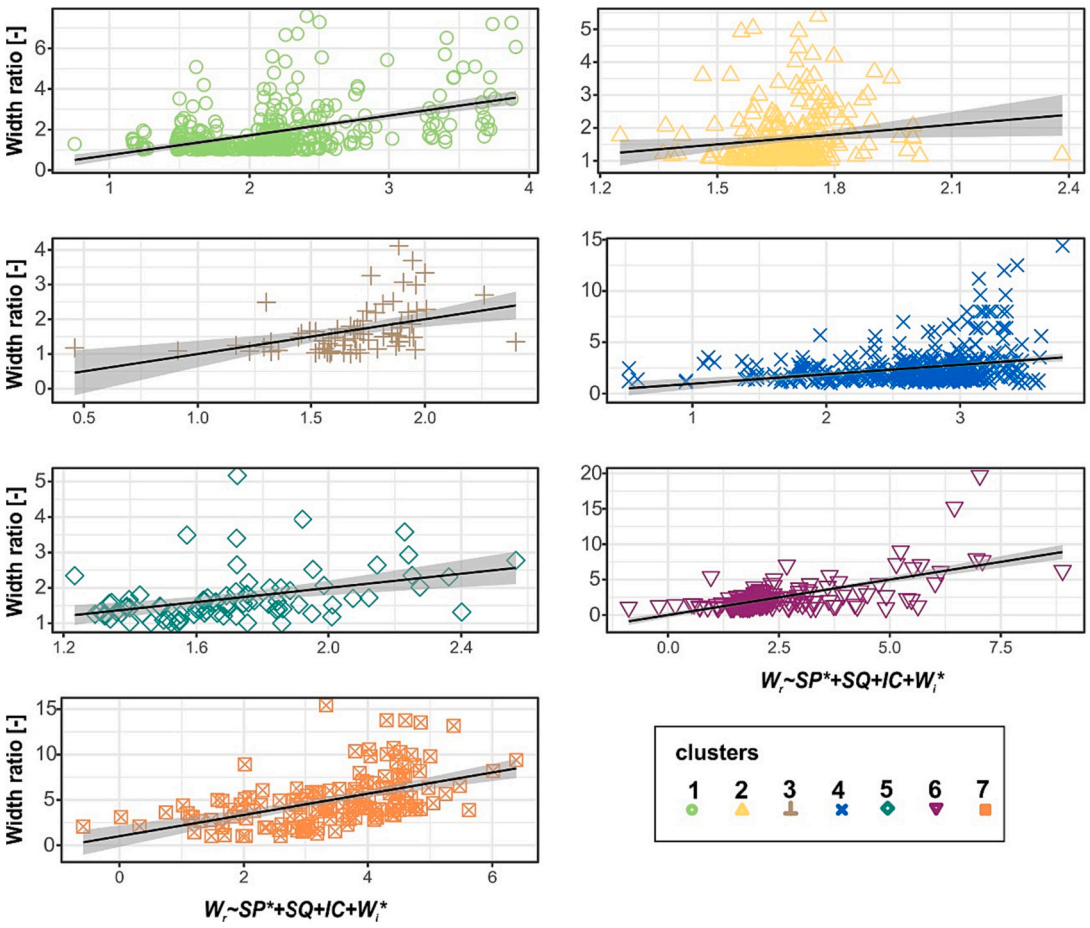

Fig. 10. Scatter plots of observed width ratio (W_r) and predicted values obtained with the multiple regression model 1 ($W_r \sim 1.90 + 4.6e\text{-}05 \cdot SP^* + 6.8e\text{-}02 \cdot SQ + 8.2e\text{-}03 \cdot IC - 1.3e\text{-}01 \cdot W_i^*$) for each cluster. The black lines show the best fit (50 % regression quantile) and 95 % confidence intervals.

effectiveness (Newson, 1980; Costa and O'Connor, 1995; Magilligan et al., 2015). Reaches of cluster 4 affected by floods triggered by longer rainfall showed larger width ratios than those affected by shorter-duration storms, in agreement with some previous observations (Gervasi et al., 2021).

We observed that reaches in the Mediterranean region (clusters 6 and 7) showed the largest width ratios. Floods in this region are usually triggered by high-intensity convective storms, generally in summer and early autumn, favoured by low-level instability and high temperatures (Gaume et al., 2016; Llasat, 2021). After the Mediterranean reaches, the Alpine rivers showed the largest width ratio. However, comparing the four clusters with Alpine reaches, we showed that reaches in cluster 4 widened significantly more than other Alpine reaches. River reaches in cluster 4 and 3 were affected by extreme floods, but they significantly differed in terms of channel size and valley confinement.

Thus, and in agreement with previous works, we found valley confinement to be one of the main morphological variables controlling channel widening (e.g., Brierley and Fryirs, 2005; Comiti et al., 2016b; Lucía et al., 2018; Sholtes et al., 2018). However, our results suggest valley confinement was not the only limiting factor. We observed a small number of confined reaches with large width ratios (i.e., reaches of cluster 1). We should stress that confined reaches in our database were those characterized by a confinement index lower than 2, which means that although constrained, some of them may still move within the valley bottom up to two times their channel width. However, confined reaches might often be steep (Wolman and Eiler, 1958), which determines high stream power and might be more susceptible to lateral erosion along the margins of the channel and benches, producing larger widening compared to downstream unconfined reaches (Thompson and Croke, 2013). Importantly, spatial changes in valley configuration and the alternation of confined and unconfined reaches, and thus of flow energy, may be vital to determining larger erosion and widening (Rogencamp and Barton, 2012). However, we could not analyse this spatial pattern and its effect on the width ratio, as we grouped similar reaches in different clusters, independently from their geographical location and upstream/downstream continuity.

Regarding channel morphological pattern, our results showed that single-thread channels of clusters 1 and 3 widened more than multi-thread ones, whereas the opposite, multi-thread braided patterns widened more, was observed in the reaches of cluster 4 (one of the clusters showing the largest width ratio values in the dataset). The complex morphological structure of braided channels requires high stream power, erodible banks, and mobile bed material, conditions usually met in environments with high sediment supply, sparse vegetation, and relatively steep slopes (Rhoads, 2020). These conditions may prevent widening during a high range of flood conditions, as those reaches of cluster 1. But, during extreme events, for example, those affecting the reaches of clusters 3 and 4, the above-mentioned conditions may favour widening.

We observed that reaches with >50 % of forested channel length widened significantly less than reaches with less vegetation. This may be explained by several causes. Vegetation not only influences bank stability at the catchment scale, but we should also consider the role of forest in soil erosion and sediment supply (Liébault and Piégay, 2002; Liébault et al., 2005; García-Ruiz, 2010). The effect of vegetation during moderate floods may reflect not only the increased resistance to erosion due to riparian vegetation but also decreased sediment supply and, thus reduced sediment transport (Merritt and Wohl, 2002). Still, extreme

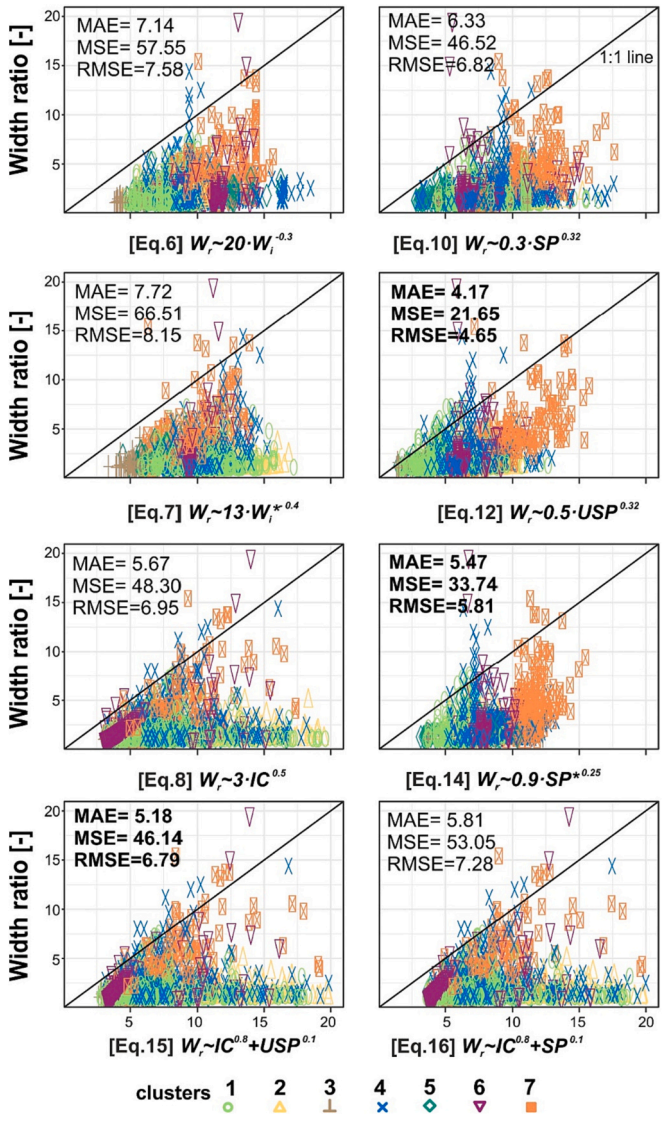

Fig. 11. Observed width ratio (W_r) versus estimated values obtained by applying the upper envelope equations shown in Table 6, for all data coloured by clusters. The black line is the 1:1 line. MAE: mean absolute error; MSE: mean standard error; RMSE: root mean squared error. *Wi*: initial channel width; W_i*: normalized width; IC: confinement index; USP: unit flood stream power; and SP*: normalized stream power. Better performance shown in bold.

floods, such as those affecting the reaches of clusters 4, 5, 6, and 7, may have enough energy to scour bank material below trees and uproot them (RenöFält et al., 2007; Smith, 2013) and transport large amounts of large wood. Our level of information for those reaches was, however, limited.

Finally, our results showed that some unconfined reaches with one reinforced bank widened more than reaches without reinforced banks during moderate floods. This reveals the important role of longitudinal discontinuous bank erosion control structures and their possible inefficiency during floods, as they can enhance erosion locally or in downstream reaches (Arnaud-Fassetta et al., 2005; Florsheim et al., 2008; Wohl, 2010).

4.3. The prediction of channel widening

Different approaches have already been proposed in the literature to predict channel widening, from rapid, regional-scale assessments, such as the exceeding critical threshold of unit stream power (Buraas et al., 2014) to more sophisticated modelling approaches (e.g., Piégay et al., 2005). Most of these previous attempts relied on hydraulic variables only (e.g., *USP* or *SP*), and were obtained for a single river or a single flood event. We provided some new insights and statistical models that may help identify reaches prone or susceptible to widening, estimating potential channel width after a flood, and computing maximum expected values of widening based on multiple variables and for different river reaches, covering a very wide range of conditions. However, we observed that the multivariate models, for example, the two dimensions from the FAMD and the three components from the PLSR, explained only 17 % and 18 % of the variance when used to predict the width ratio, respectively. Some models performed better for some of the subsets. Model 1 (Section 3.4) showed the most significant R^2 values for cluster 7 ($R^2 = 0.42$), cluster 6 ($R^2 = 0.42$), and cluster 1 ($R^2 = 0.24$), while it showed very low values for the other clusters. This could be explained because reaches in clusters 6 and 7 showed considerable width ratios, and the variables included in the multivariate models could explain relatively well the river response, whereas, in the case of reaches of other clusters, it was not the case, and the models significantly overestimated the observed width ratios. This indicates that the selected variables could not explain a large amount of variance in the data, mainly related to low width ratios (e.g., clusters 2, 3, and 5). The previous section has already mentioned some additional variables to be considered in other models. One important limitation is that these statistical models rely on the SP or related variables at the reach where widening was observed, and we did not consider the effect of the spatial variations in stream power (Baker and Costa, 1987; Magilligan et al., 2015), or gradients within reaches where a large drop in stream power may occur relative to upstream, possibly enhancing widening (Sholtes et al., 2018). This, as explained in the previous section for changes in the valley confinement, could not be evaluated and would deserve additional analyses.

Channel widening is the result of a complex set of interacting natural processes that are highly variable in nature. It is, therefore, not surprising that width ratios range over several orders of magnitude. Yet, the ability of some models to represent >40 % of the variation in the observed width ratios in our dataset is encouraging, considering the diversity of conditions and the complexity of the processes involved.

While focusing on the large W_r values may be essential, in the case of very wide rivers, low width ratios may also mean several tens of meters of channel widening. For example, the reaches of cluster 3 (initial mean channel width > 50 m) showed width ratios up to 4 (widening >100 m). The apparently low width ratio may give a false sense of marginal planform change in these reaches. By proposing upper bound widening ratios, we can overcome this limitation. The envelope curves obtained from the quantile regression showed that they fitted well to the large values of the observed width ratios for all clusters in our dataset. Thus, they are helpful to identify reaches potentially prone to large widening and getting first-order estimates of the maximum expected width ratio. Applying upper boundaries is common in other fields (e.g., Guzzetti et al., 2008; O'Connor et al., 2013; Marchi et al., 2016; Yu et al., 2022). Upper envelopes to predict channel widening were proposed by Comiti et al. (2016b), who stressed the caution needed when applying such approaches, as they were obtained by analysing a much smaller database, limited to one river basin and to one flood event. Here, by extending the database to several rivers, thousands of reaches, and multiple floods of different magnitude, we provide a robust set of equations that could be applied according to the specific river types identified in our database, the flood type, and to the available information (i.e., discharge, *USP*, *IC*, etc.).

4.4. Importance for flood hazard and risk assessment and river restoration

Predicting where significant geomorphic changes will occur during floods would be of utmost importance for characterizing flood hazard zones and informing the management of river basins. Therefore, there is

a need to include channel widening in flood hazard assessment effectively. On the other hand, it could be equally important to identify dynamic river reaches with a high potential for passive restoration (Kondolf, 2011).

The definition of an erodible corridor based on historical maps or topography has been proved beneficial to delineate the extent of the valley bottom that might be susceptible to planform changes (Piégay et al., 2005; Hajdukiewicz and Wyżga, 2023). These techniques, however, require high-resolution information to be analysed and are generally suitable for more extended time scales. Our results can be used as a quicker first-order approach to identify reaches susceptible to extensive widening and to predict the worst-case scenario of channel widening by, for example, applying the upper-envelope equations reported in Table 3. The combination of the delineation of erodible corridors and the zones susceptible to planform changes with more detailed analyses, like numerical modelling, or the application of stochastic approaches (e.g., Zerfu et al., 2015) together with the upper envelopes, would also allow assessing uncertainties better and could be used to predict the longer-term evolution of river trajectories.

5. Conclusions

This work used a large dataset of 1564 river reaches from 51 rivers that experienced channel widening after floods of different magnitudes and frequencies and were located in different regions and climatic settings in Europe. We identified seven groups of reaches with significantly different responses to floods in terms of width ratios. The study shows that extreme floods triggered by short and intense precipitation events in fairly steep basins were responsible for larger widening, particularly those analysed reaches located in the Mediterranean region. Still, the role of moderate flood in producing significant widening has also been illustrated. Valley confinement was one of the main morphological variables controlling channel widening, but not always the only limiting factor, according to our findings. We proposed new statistical models that may help identify reaches susceptible to widening, estimate potential channel width after a flood, and compute upper-bound widening. Therefore, they can be used to inform flood hazard evaluations and help the design of mitigation measures, and river management in general, including river restoration.

CRediT authorhip contribution statement

Ruiz-Villanueva, V. Conceptualization; Data acquisition, Data curation; Formal analysis; Methodology; Writing – original draft; Writing – review & editing.

Piégay, H. Conceptualization; Methodology; Writing – review & editing.

Scorpio, V. Data acquisition, Conceptualization; Methodology; Writing – review & editing.

Bachmann, A. Data acquisition.

Brousse, G. Data acquisition.

Cavalli, M. Writing – review & editing.

Comiti, F. Conceptualization; Methodology; Writing – review & editing.

Crema, S. Writing – review & editing.

Fernández, E. Data acquisition, Writing – review & editing.

Furdada, G. Data acquisition, Writing – review & editing.

Hajdukiewicz, H. Data acquisition, Writing – review & editing.

Hunzinger, L. Data acquisition, Writing – review & editing.

Lucía, A. Data acquisition, Writing – review & editing.

Marchi, L. Conceptualization; Methodology; Writing – review & editing.

Moraru, A. Data acquisition, Writing – review & editing.

Piton, G. Conceptualization; Methodology; Writing – review & editing.

Rickenmann, D. Conceptualization; Methodology; Writing – review & editing.

Righini, M. Data acquisition, Writing – review & editing.

Surian, N. Conceptualization; Methodology; Writing – review & editing.

Yassine, R. Data acquisition, Writing – review & editing.

Wyżga, B. Conceptualization; Methodology; Writing – review & editing.

Declaration of competing interest

The authors declare that they have no known competing financial interests or personal relationships that could have appeared to influence the work reported in this paper.

Data availability

Data will be made available on request.

Acknowledgments

The participation of V.RV was funded by the Swiss National Science Foundation (SNSF; grant no. PCEFP2_186963); and G.P. was funded by the H2020 project NAIAD (grant no. 730497) from the European Union's Horizon 2020 research and innovation program. We would like to dedicate this work to the memory of Bartłomiej Wyżga, who actively contributed to early versions of the manuscript. Thanks to the eight reviewers who provided comments and helped improve the manuscript.

Appendix A. Supplementary data

Supplementary data to this article can be found online at https://doi.org/10.1016/j.scitotenv.2023.166103.

References

Abernethy, B., Rutherfurd, I.D., 2001. The distribution and strength of riparian tree roots in relation to riverbank reinforcement. Hydrol. Process. 15, 63–79.

Alber, A., Piégay, H., 2017. Characterizing and modelling river channel migration rates at a regional scale: case study of south-east France. J. Environ. Manag. 202, 479–493. https://doi.org/10.1016/j.jenvman.2016.10.055.

Amponsah, W., 2017. Stream Power and Geomorphic Effects of Flash Floods. PhD Thesis. University of Padova (166 pp.).

Amponsah, W., Marchi, L., Zoccatelli, D., Boni, G., Cavalli, M., Comiti, F., Crema, S., Lucía, A., Marra, F., Borga, M., 2016. Hydrometeorological characterisation of a flash flood associated with major geomorphic effects: assessment of peak discharge uncertainties and analysis of the runoff response. J. Hydrometeorol. 17, 3063–3077. https://doi.org/10.1175/JHM-D-16-0081.1.

Anderson, H.W., 1957. Relating sediment yield to catchment area variables. Trans. Am. Geophys. Union 38 (6), 921–924.

Arnaud, F., Piégay, H., Schmitt, L., Rollet, A.J., Ferrier, V., Béal, D., 2015. Historical geomorphic analysis (1932–2011) of a by-passed river reach in process-based restoration perspectives: the Old Rhine downstream of the Kembs diversion dam (France Germany). Geomorphology 236, 163–177.

Arnaud-Fassetta, G., Cossart, E., Fort, M., 2005. Hydro-geomorphic hazards and impact of man-made structures during the catastrophic flood of June 2000 in the Upper Guil catchment (Queyras, French Alps). Geomorphology 66, 41–67.

Bachmann, W.A., 2012. Ausmass und auftreten von seitenerosionen bei hochwasserereignissen. Master Thesis. Universität Bern (157pp. Unpublished. (In German)).

Badoux, A., Andres, N., Turowski, J.M., 2014. Damage costs due to bedload transport processes in Switzerland. Nat. Hazards Earth Syst. Sci. 14, 279–294. https://doi.org/10.5194/nhess-14-279-2014.

Baker, V., Costa, J., 1987. Flood power. In: Baker, V., Costa, J. (Eds.), Catastrophic Flooding. George Allen and Unwin, London, pp. 1–21.

Bednarska, A., Wyżga, B., Mikuś, P., Kędzior, R., 2018. Ground beetle communities in a mountain river subjected to restoration. Sci. Total Environ. 610–611, 1180–1192. https://doi.org/10.1016/j.scitotenv.2017.07.161.

Beechie, T.J., Sear, D.A., Olden, J.D., Pess, G.R., Buffington, J.M., Moir, H., Roni, P., Pollock, M.M., 2010. Process-based principles of restoring river ecosystems. BioScience 60, 209–222.

Belletti, B., Durfour, S., Piégay, H., 2014. Regional assessment of the multi-decadal changes in braided riverscapes following large floods (example of 12 reaches in South East of France). Adv. Geosci. 37, 57–71. https://doi.org/10.5194/adgeo-37-57-2014.

Bertrand, M., Liébault, F., 2019. Active channel width as a proxy of sediment supply from mining sites in New Caledonia. Earth Surf. Process. Landf. 44 (1), 67–76. https://doi.org/10.1002/esp.4478.
Beven, K., 1981. The effect of ordering on the geomorphic effectiveness of hydrologic events. In: Davies, T.R.H., Pearce, A.J. (Eds.), Erosion and Sediment Transport in the Pacific Rim Steeplands. IAHS Publication, vol. No. 132. IAHS Press, Wallingford, UK, pp. 510–526.
Biron, P.M., Buffin-Bélanger, T., Larocque, M., Choné, G., Cloutier, C.-A., Ouellet, M.-A., Demers, S., Olsen, T., Desjarlais, C., Eyquem, J., 2014. Freedom space for rivers: a sustainable management approach to enhance river resilience. Environ. Manag. 54 (5), 1056–1073.
Brenna, A., Marchi, L., Borga, M., Zaramella, M., Surian, N., 2023. What drives major channel widening in mountain rivers during floods? The role of debris floods during a high-magnitude event. Geomorphology 430, 108650. https://doi.org/10.1016/j.geomorph.2023.108650.
Brierley, G.J., Fryirs, K.A., 2005. Geomorphology and River Management. Applications of the River Styles Framework. Blackwell, Oxford (398 pp).
Brierley, G.J., Fryirs, K.A., Boulton, A., Cullum, C., 2008. Working with change: the importance of evolutionary perspectives in framing the trajectory of river adjustment. In: Brierley, G.J., Fryirs, K.A. (Eds.), River Futures: An Integrative Scientific Approach to River Repair, p. 65.
Brousse, G., Arnaud-Fassetta, G., Cordier, S., 2011. Evolution hydrogéomorphologique de la bande active de l'Ubaye (Alpes françaises du Sud) de 1956 à 2004: contribution à la gestion des crues. In: Géomorphologie: relief, processus, environnement, 3, pp. 307–318 (In French).
Brunsden, D., 2001. A critical assessment of the sensitivity concept in geomorphology. Catena 42, 99–123. https://doi.org/10.1016/S0341-8162(00)00134-X.
Buffin-Bélanger, T., Biron, P.M., Larocque, M., Demers, S., Olsen, T., Chone, G., Ouellet, M.-A., Cloutier, C.-A., Desjarlais, C., Eyquem, J., 2015. Freedom space for rivers: an economically viable river management concept in a changing climate. Geomorphology 251, 137–148. https://doi.org/10.1007/s00267-014-0366-z.
Buraas, E.M., Renshaw, C.E., Magilligan, F.J., Dade, W.B., 2014. Impact of reach geometry on stream channel sensitivity to extreme floods. Earth Surf. Process. Landf. 39, 1778–1789.
Comiti, F., Lucía, A., Rickenmann, D., 2016a. Large wood recruitment and transport during large floods: a review. Geomorphology 269, 23–39.
Comiti, F., Righini, M., Nardi, L., Lucía, A., Amponsah, W., Cavalli, M., Surian, N., 2016b. Channel widening during extreme floods: how to integrate it within river corridor planning? 13th Congress Interpraevent 2016. Lucerne (Switzerland) 477–486.
Costa, J.E., O'Connor, J.E., 1995. Geomorphically effective floods. In: Costa, J.E., Miller, A.J., Potter, K.W., Wilcock, P.R. (Eds.), Natural and Anthropogenic Influences in Fluvial Geomorphology. American Geophysical Union, Washington, DC.
Dean, D.J., Schmidt, J.C., 2013. The geomorphic effectiveness of a large flood on the Rio Grande in the Big Bend region: insights on geomorphic controls and post-flood geomorphic response. Geomorphology 201, 183–198.
Dufour, S., Piégay, H., 2009. From the myth of a lost paradise to targeted river restoration: forget natural references and focus on human benefits. River Res. Appl. 25 (5), 568–581.
Eager, C.D., 2017. Standardize: Tools for Standardizing Variables for Regression in R. R package version 0.2.1. https://CRAN.R-project.org/package=standardize.
European Environmental Agency, 2016. https://www.eea.europa.eu/data-and-maps/data/biogeographical-regions-europe-3#tab-metadata.
Felix De Almeida, I., Yassine, R., 2018. Analyse historique sur le bassin versant du Gave de Pau amont, Technical report. Pays de Lourdes et des Vallées des Gaves (PLVG).
Feng, D., Gleason, C.J., Yang, X., Allen, G.H., Pavelsky, T.M., 2022. How have global river widths changed over time? Water Resour. Res. 58, e2021WR031712 https://doi.org/10.1029/2021WR031712.
Fernández Iglesias, E., Marquínez, J., 2013. Aplicación de criterios geomorfológicos e históricos de detalle para la delimitación del DPHP en la cuenca del Ebro. Informe inédito INDUROT para la CHEbro (38 pp.).
Florsheim, J.L., Mount, J.F., Chin, A., 2008. Bank erosion as a desirable attribute of rivers. BioScience 58, 519–529.
Fratkin, M.M., Segura, C., Bywater-Reyes, S., 2020. The influence of lithology on channel geometry and bed sediment organization in mountainous hillslope-coupled streams. Earth Surf. Process. Landf. 45, 2365–2379. https://doi.org/10.1002/esp.4885.
Fryirs, K., Lisenby, P., Croke, J., 2015. Morphological and historical resilience to catastrophic flooding: the case of Lockyer Creek, SE Queensland, Australia. Geomorphology 241, 55–71.
García-Ruiz, J.M., 2010. The effects of land uses on soil erosion in Spain: a review. Catena 81, 1–11.
Gaume, E., Borga, M., Llassat, M.C., Maouche, S., Lang, M., Diakakis, M., 2016. Mediterranean extreme floods and flash floods (Sub-chapter 1.3.4). In: Allenvi (Ed.), The Mediterranean Region Under Climate Change. A Scientific Update, Coll. Synthèses, IRD Editions, pp. 133–144.
Gervasi, A.A., Pasternack, G.B., East, A.E., 2021. Flooding duration and volume more important than peak discharge in explaining 18 years of gravel–cobble river change. Earth Surf. Process. Landf. 46, 3194–3212. https://doi.org/10.1002/esp.5230.
Guzzetti, F., Peruccacci, S., Rossi, M., Stark, C.P., 2008. The rainfall intensity-duration control of shallow landslides and debris flows: an update. Landslides 5 (1), 3–17. https://doi.org/10.1007/s10346-007-0112-1.
Hajdukiewicz, H., Wyżga, B., 2023. Analysis of historical changes in planform geometry of a mountain river to inform design of erodible river corridor. Ecol. Eng. 186, 106821 https://doi.org/10.1016/j.ecoleng.2022.106821.
Hajdukiewicz, H., Wyżga, B., Mikuś, P., Zawiejska, J., Radecki-Pawlik, A., 2016. Impact of a large flood on mountain river habitats, channel morphology, and valley infrastructure. Geomorphology 272, 55–67. https://doi.org/10.1016/j.geomorph.2015.09.003.
Hajdukiewicz, H., Wyżga, B., Zawiejska, J., 2019. Twentieth century hydromorphological degradation of Polish Carpathian rivers. Quat. Int. 504, 181–194. https://doi.org/10.1016/j.quaint.2017.12.011.
Hao, L., Naiman, D.Q., 2007. Quantile Regression. Sage Publications, London.
Harvey, A.M., 1991. The influence of sediment supply on the channel morphology of upland streams: Howgill Fells, Northwest England. Earth Surf. Process. Landforms 16, 675–684. https://doi.org/10.1002/esp.3290160711.
Harvey, A.M., 2001. Coupling between hillslopes and channels in upland fluvial systems: implications for landscape sensitivity, illustrated from the Howgill Fells, northwest England. Catena 42, 225–250.
Hey, R., Thorne, C., 1986. Stable channels with mobile gravel beds. J. Hydraul. Eng. 112, 671–689. https://doi.org/10.1061/(ASCE)0733-9429(1986)112:8(671).
Hickin, E.J., 1984. Vegetation and river channel dynamics. In: Canadian Geographer/Le.
Hohensinner, S., Egger, G., Muhar, S., Vaudor, L., Piégay, H., 2021. What remains today of pre-industrial alpine rivers? Census of historical and current channel patterns in the Alps. River Res. Appl. 37, 128–149. https://doi.org/10.1002/rra.3751.
Hooke, J.M., 1979. An analysis of the processes of river bank erosion. J. Hydrol. 42 (1–2), 39–62. https://doi.org/10.1016/0022-1694(79)90005-2.
Hunzinger, L., Durrer, S., 2009. Ereignisanalyse Hochwasser 2005: Seitenerosion. In: Bezzola, G.R., Hegg, C. (Eds.), Ereignisanalyse Hochwasser 2005, Teil 2- Analyse von Prozessen, Massnahmen und Gefahrengrundlgen. Bundesamt für Umwelt BAFU, Eidgenössische Forschungsanstalt WSL, Umwelt-Wissen Nr. 0825. Bern, pp. 1–159 (In German).
Husson, F., Josse, J., Pagès, J., 2010. Principal Component Methods-Hierarchical Clustering-Partitional Clustering: Why Would We Need to Choose for Visualizing Data? (Unpublished Data). http://www.sthda.com/english/upload/hcpc_husson_josse.pdf.
Kassambara, A., 2017. HCPC-Hierarchical Clustering on Principal Components: Essentials. Available: http://www.sthda.com/english/articles/31-principal-component-methods-in-r-practical-guide/117-hcpc-hierarchical-clustering-on-principal-components-essentials/.
Kassambara, A., Mundt, F., 2020. Factoextra: Extract and Visualize the Results of Multivariate Data Analyses. R package version 1.0.7. https://CRAN.R-project.org/package=factoextra.
Kline, M., Cahoon, B., 2010. Protecting river corridors in Vermont. J. Am. Water Resour. Assoc. 46 (2), 227–236.
Koenker, R., 2005. Quantile Regression. Cambridge University Press, New York.
Koenker, R., 2022. quantreg: Quantile Regression. R package version 5.93. https://CRAN.R-project.org/package=quantreg.
Koenker, R., Park, B.J., 1994. An interior point algorithm for nonlinear quantile regression. J. Econ. 71 (1–2), 265–283.
Kondolf, M. G. 2011. Setting goals in river restoration: when and where can the river "heal itself"?. In: Book Editor(s): Andrew Simon, Sean J. Bennett, Janine M. Castro. Stream Restoration in Dynamic Fluvial Systems: Scientific Approaches, Analyses, and Tools, volume 194. doi:https://doi.org/10.1029/2010GM001020.
Krapesch, G., Hauer, C., Habersack, H., 2011. Scale orientated analysis of river width changes due to extreme flood hazards. Nat. Hazards Earth Syst. Sci. 11, 2137–2147. https://doi.org/10.5194/nhess-11-2137-2011.
Kuentz, A., Arheimer, B., Hundecha, Y., Wagener, T., 2017. Understanding hydrologic variability across Europe through catchment classification. Hydrol. Earth Syst. Sci. 21, 2863–2879. https://doi.org/10.5194/hess-21-2863-2017.
Lawler, D.M., 1993. The measurement of river bank erosion and lateral channel change: a review. Earth Surf. Process. Landf. 18, 777–821. https://doi.org/10.1002/esp.3290180905.
Lê, S., Josse, J., Husson, F., 2008. FactoMineR: a package for multivariate analysis. J. Stat. Softw. 25 (1), 1–18. https://doi.org/10.18637/jss.v025.i01.
Liébault, F., Piégay, H., 2002. Causes of 20th century channel narrowing in mountain and piedmont rivers of southeastern France. Earth Surf. Process. Landf. 27 (4), 425–444. https://doi.org/10.1002/esp.328.
Liébault, F., Gomez, B., Page, M., Marden, M., Peacock, D., Richard, D., Trotter, C.M., 2005. Land-use change, sediment production and channel response in upland regions. River Res. Appl. 21 (7), 739–756. https://doi.org/10.1002/rra.880.
Liland, K.H., Mevik, B., Wehrens, R., 2022. pls: Partial Least Squares and Principal Component Regression. R package version 2.8-1. https://CRAN.R-project.org/package=pls.
Llasat, M.C., 2021. Floods evolution in the Mediterranean region in a context of climate and environmental change. Cuadernos de Investigación Geografica CIG 47 (1), 13–32. https://publicaciones.unirioja.es/ojs/index.php/cig/article/view/4897.
Lucía, A., Schwientek, M., Eberle, J., Zarfl, C., 2018. Planform changes and large wood dynamics in two torrents during a severe flash flood in Braunsbach, Germany 2016. Sci. Total Environ. 640–641, 315–326. https://doi.org/10.1016/j.scitotenv.2018.05.186.
Magilligan, F.J., Buraas, E.M., Renshaw, C.E., 2015. The efficacy of stream power and flow duration on geomorphic responses to catastrophic flooding. Geomorphology 228, 175–188. https://doi.org/10.1016/j.geomorph.2014.08.016.
Marchi, L., Cavalli, M., Amponsah, W., Borga, M., Crema, S., 2016. Upper limits of flash flood stream power in Europe. Geomorphology 272 (1), 68–77. https://doi.org/10.1016/j.geomorph.2015.11.005.
Marquínez, J., Fernández Iglesias, E., Arnal, J.M., Moreno, M.L., 2014. Reactivación del cauce histórico del río Ésera por la avenida de Junio de 2013 (Pirineo Central). XIII Reunión Nacional de Geomorfología, Cáceres, pp. 115–118.
Martin, M., 2021. sfsmisc: Utilities from 'Seminar fuer Statistik' ETH Zurich. R package version 1.1-12. https://CRAN.R-project.org/package=sfsmisc.

Merritt, D.M., Wohl, E.E., 2002. Processes governing hydrochory along rivers: hydraulics, hydrology, and dispersal phenology. Ecol. Appl. 12, 1071–1087. https://doi.org/10.1890/1051-0761(2002)012[1071:PGHARH]2.0.CO;2.
Mevik, B., Wehrens, R., 2007. The pls package: principal component and partial least squares regression in R. J. Stat. Softw. 18 (2), 1–24.
Mevik, B., Wehrens, R., 2022. Introduction to the pls package. Pls manual. https://cran.r-project.org/web/packages/pls/vignettes/pls-manual.pdf.
Milan, D.J., 2012. Geomorphic impact and system recovery following an extreme flood in an upland stream: Thinhope Burn, northern England, UK. Geomorphology 138, 319–328.
Nardi, L., Rinaldi, M., 2015. Spatio-temporal patterns of channel changes in response to a major flood event: the case of the Magra River (central-northern Italy). Earth Surf. Process. Landf. 40, 326–339. https://doi.org/10.1002/esp.3636.
Newson, M.D., 1980. The geomorphological effectiveness of floods: a contribution stimulated by two recent events in mid-Wales. Earth Surface Processes 5, 1–16.
Ockelford, A., Woodcock, S., Haynes, H., 2019. The impact of inter-flood duration on non-cohesive sediment bed stability. Earth Surf. Process. Landf. 44 (14), 2861–2871. https://doi.org/10.1002/esp.4713.
O'Connor, J.E., Clague, J.J., Walder, J.S., Manville, V., Beebee, R.A., 2013. Chapter 9.25 Outburst Floods, In: Editor(s): John F. Shroder, Treatise on Geomorphology. Academic Press, pp. 475–510 (ISBN 9780080885223). https://doi.org/10.1016/B978-0-12-374739-6.00251-7.
Perignon, M.C., Tucker, G.E., Griffin, E.R., Friedman, J.M., 2013. Effects of riparian vegetation on topographic change during a large flood event, Rio Puerco, New Mexico USA. J. Geophys. Res. Earth Surf. 118, 1193–1209. https://doi.org/10.1002/jgrf.20073.
Pfeiffer, A.M., Finnegan, N.J., Willenbring, J.K., 2017. Sediment supply controls equilibrium channel geometry in gravel rivers. Proc. Natl. Acad. Sci. U. S. A. 114, 3346–3351. https://doi.org/10.1073/pnas.1612907114.
Piégay, H., Darby, S.E., Mosselman, E., Surian, N., 2005. A review of techniques available for delimiting the erodible river corridor: a sustainable approach to managing bank erosion. River Res. Appl. 21, 773–789. https://doi.org/10.1002/rra.881.
Piégay, H., Alber, A., Slater, L., Bourdin, L., 2009. Census and typology of braided rivers in the French Alps. Aquat. Sci. 71, 371–388. https://doi.org/10.1007/s00027-009-9220-4.
Piton, G., Recking, A., 2019. Steep bedload-laden flows: near critical? J. Geophys. Res. Earth Surf. 124 (8), 2160–2175. https://doi.org/10.1029/2019JF005021.
Piton, G., Dupire, S., Arnaud, P., Mas, A., Marchal, R., Moncoulon, D., Curt, T., Tacnet, J., 2018. DELIVERABLE 6.2 from hazards to risk: models for the DEMOs-part 3: France: Brague catchment DEMO. NAIAD H2020 project (Grant agreement n° 730497), 101 pp. [online]. Available at. http://naiad2020.eu/wp-content/uploads/2019/02/D6.2_REV_FINAL.pdf.
Pollen, N., 2007. Temporal and spatial variability in root reinforcement of streambanks: accounting for soil shear strength and moisture. Catena 69, 197–205. https://doi.org/10.1016/j.catena.2006.05.004.
Pollen, N., Simon, A., Collison, A., 2004. Advances in assessing the mechanical and hydrologic effects of riparian vegetation on streambank stability. In: Bennett, S.J., Simon, A. (Eds.), Riparian Vegetation and Fluvial Geomorphology: Water Science and Application. American Geophysical Union, Washington, D.C, pp. 125–139.
R Core Team, 2021. R: A Language and Environment for Statistical Computing. R Foundation for Statistical Computing, Vienna, Austria. URL. https://www.R-project.org/.
R Studio Team, 2018. Rstudio: Integrated Development for R. Rstudio, Inc., Boston, MA. URL. http://www.rstudio.com/.
Rapp, C.F., Abbe, T.B., 2003. A framework for delineating channel migration zones. In: Washington State Departments of Ecology and of Transportation, Ecology Publication #03-06-027, 66 pp. and 5 appendix. Available at: https://fortress.wa.gov/ecy/publications/documents/0306027.pdfE.
RenöFält, B.M., Merritt, D.M., Nilsson, C., 2007. Connecting variation in vegetation and stream flow: the role of geomorphic context in vegetation response to large floods along Boreal Rivers. J. Appl. Ecol. 44 (1), 147–157.
Rhoads, B.L., 2020. River Dynamics: Geomorphology to Support Management. Cambridge University Press (526pp. ISBN: 9781107195424).
Rickenmann, D., Badoux, A., Hunzinger, L., 2016. Significance of sediment transport processes during piedmont floods: the 2005 flood events in Switzerland. Earth Surf. Process. Landf. 41, 224–230. https://doi.org/10.1002/esp.3835.
Righini, M., Surian, N., Wohl, E., Marchi, L., Comiti, F., Amponsah, W., Borga, M., 2017. Geomorphic response to an extreme flood in two Mediterranean rivers (northeastern Sardinia, Italy): analysis of controlling factors. Geomorphology 290, 184–199. https://doi.org/10.1016/j.geomorph.2017.04.014.
Rogencamp, G., Barton, J., 2012. The Lockyer Creek flood of January 2011: what happened and how should we manage hazard for rare floods. In: 52nd Annual Floodplain Management Authorities Conference, 21st -24th February 2012, Batemans Bay, NSW.
Rohde, S., Schütz, M., Kienast, F., Englmaier, P., 2005. River widening: an approach to restoring riparian habitats and plant species. River Res. Applic. 21, 1075–1094. https://doi.org/10.1002/rra.870.
Rohde, S., Hostmann, M., Peter, A., Ewald, K.C., 2013. Room for rivers: An integrative search strategy for floodplain restoration. In: Landscape and Urban Planning, Volume 78, Issues 1–2, 15 October 2006, pp. 50–70. https://doi.org/10.1016/j.landurbplan.2005.05.006.
Rubel, F., Kottek, M., 2010. Observed and projected climate shifts 1901-2100 depicted by world maps of the Köppen-Geiger climate classification. Meteorol. Z. 19 (2), 135–141. https://doi.org/10.1127/0941-2948/2010/0430.
Ruiz-Villanueva, V., Badoux, A., Rickenmann, D., Böckli, M., Schläfli, S., Steeb, N., Stoffel, M., Rickli, C., 2018. Impacts of a large flood along a mountain river basin: the importance of channel widening and estimating the large wood budget in the upper Emme River (Switzerland). Earth Surface Dynamics 6, 1115–1137. https://doi.org/10.5194/esurf-2018-44.
Scorpio, V., Piégay, H., 2021. Is afforestation a driver of change in italian rivers within the Anthropocene era? Catena 198, 105031 (ISSN 0341-8162). https://doi.org/10.1016/j.catena.2020.105031.
Scorpio, V., Aucelli, P.P.C., Giano, I., Pisano, L., Robustelli, G., Rosskopf, C.M., Schiattarella, M., 2015. River channel adjustment in southern Italy over the past 150 years and implications for channel recovery. Geomorphology 251, 77–90. https://doi.org/10.1016/j.geomorph.2015.07.008.
Scorpio, V., Crema, S., Marrad, F., Righini, M., Ciccarese, G., Borga, M., Cavalli, M., Corsini, A., Marchi, L., Surian, N., Comiti, F., 2018. Basin-scale analysis of the geomorphic effectiveness of flash floods: a study in the northern Apennines (Italy). Sci. Total Environ. 640–641, 337–351. https://doi.org/10.1016/j.scitotenv.2018.05.252.
Scorpio, V., Cavalli, M., Steger, S., Crema, S., Marra, F., Zaramella, M., Borga, M., Marchi, L., Comiti, F., 2022. Storm characteristics dictates sediment dynamic and geomorphic changes in mountain channels: a case study in the Italian Alps. Geomorphology 403, 108173. Available from: https://doi.org/10.1016/j.geomorph.2022.108173.
Segura-Beltrán, F., Sanchis-Ibor, C., 2013. Assessment of channel changes in a Mediterranean ephemeral stream since the early twentieth century: the Rambla de Cervera, eastern Spain. Geomorphology 201, 199–214.
Shields, A., 1936. Anwendung der Ähnlichkeitsmechanik und der Turbulenzforschung auf die Geschiebebewe-gung [application of similarity principles and turbulence research to bedload movement]. In: Mitteilungen der Preußischen Versuchsanstalt für Wasserbau und Schiffbau, Berlin, vol. 26 (26 pp.).
Sholtes, J.S., Yochum, S.E., Scott, J.A., Bledsoe, B.P., 2018. Longitudinal variability of geomorphic response to floods. Earth Surf. Proc. Land. 43, 3099–3113.
Smith, B., 2013. The Role of Vegetation in Catastrophic Floods: A Spatial Analysis, Bachelor of Environmental Science (Honours). School of Earth & Environmental Science, University of Wollongong. http://ro.uow.edu.au/thsci/65.
Surian, N., Rinaldi, M., Pellegrini, L., Audisio, C., Maraga, F., Teruggi, L., Ziliani, L., 2009. Channel adjustments in northern and Central Italy over the last 200 years. Geol. Soc. Am. Spec. Pap. 451, 83–95.
Surian, N., Righini, M., Lucía, A., Nardi, L., Amponsah, W., Benvenuti, M., Borga, M., Cavalli, M., Comiti, F., Marchi, L., Rinaldi, M., Viero, A., 2016. Channel response to extreme floods: insights on controlling factors from six mountain rivers in northern Apennines, Italy. Geomorphology 272, 78–91. https://doi.org/10.1016/j.geomorph.2016.02.002.
Surian, N., Brenna, A., Borga, M., Cavalli, M., Comiti, F., Marchi, L., Zaramella, M., 2020. Flood Hazard in Mountain Streams: The Key Role of Geomorphic Processes during High Magnitude Events, EGU General Assembly 2020, Online, 4–8 May 2020, EGU2020–9682. https://doi.org/10.5194/egusphere-egu2020-9682.
Thompson, C., Croke, J., 2013. Geomorphic effects, flood power, and channel competence of a catastrophic flood in confined and unconfined reaches of the upper Lockyer valley, Southeast Queensland, Australia. Geomorphology 197, 156–169.
Török, G.T., Parker, G., 2022. The influence of riparian woody vegetation on bankfull alluvial river morphodynamics. Sci. Rep. 1–15 https://doi.org/10.1038/s41598-022-22846-1.
Vaissie, A.M., Husson, F., 2021. Factoshiny: Perform Factorial Analysis from 'FactoMineR' with a Shiny Application. R package version 2.4. https://CRAN.R-project.org/package=Factoshiny.
Vargas-Luna, A., Duró, G., Crosato, A., Uijttewaal, W., 2019. Morphological adaptation of river channels to vegetation establishment: a laboratory study. J. Geophys. Res. Earth Surf. 124 (7), 1981–1995. https://doi.org/10.1029/2018JF004878.
Whitbread, K., Jansen, J., Bishop, P., Attal, M., 2015. Substrate, sediment, and slope controls on bedrock channel geometry in postglacial streams. J. Geophys. Res. Earth Surf. 120, 779–798. https://doi.org/10.1002/2014JF003295.
Williams, G.P., Wolman, M.G., 1984. Downstream effects of dams on alluvial rivers. USGS Numbered Series 1286. https://doi.org/10.3133/pp1286.
Wohl, E.E., 2010. Mountain Rivers revisited. In: Book Series Water Resources Monograph. Am. Geophys. Union, 19 (573 pp.). Print ISBN:9780875903231. Online ISBN:9781118665572. DOI:10.1029/WM019.
Wohl, E., Merritt, D.M., 2008. Reach-scale channel geometry of mountain streams. Geomorphology 93, 168–185. https://doi.org/10.1016/j.geomorph.2007.02.014.
Wohl, E.E., Bledsoe, B.P., Jacobson, R.B., Poff, N.L., Rathburn, S.L., Walters, D.M., Wilcox, A.C., 2015. The natural sediment regime in Rivers: broadening the Foundation for Ecosystem Management. BioScience 65 (4), 358–371. https://doi.org/10.1093/biosci/biv002.
Wolman, M.G., Eiler, J.P., 1958. Reconnaissance study of erosion and deposition produced by the flood of August 1955 in Connecticut: American Geophysical Union Transactions, 39, pp. 1–14. https://doi.org/10.1029/TR039i001p00001.
Wolman, M.G., Gerson, R., 1978. Relative scales of time and effectiveness of climate in water- shed geomorphology: Earth Surface Processes, 3, pp. 189–208.
Wyżga, B., Zawiejska, J., Hajdukiewicz, H., 2016. Multi-thread rivers in the Polish Carpathians: occurrence, decline and possibilities of restoration. Quat. Int. 415, 344–356. https://doi.org/10.1016/j.quaint.2015.05.015.
Yousefi, S., Mirzaee, S., Keesstra, S., Surian, N., Pourghasemi, H.R., Zakizadeh, H.R., Tabibian, S., 2018. Effects of an extreme flood on river morphology (case study:

Karoon River, Iran). Geomorphology 304, 30–39. https://doi.org/10.1016/j.geomorph.2017.12.034 (ISSN 0169-555X).

Yu, G., Wright, D.B., Davenport, F.V., 2022. Diverse physical processes drive upper-tail flood quantiles in the US mountain west. Geophys. Res. Lett. 49, e2022GL098855 https://doi.org/10.1029/2022GL098855.

Zerfu, T., Beevers, L.C., Crosato, A., Wright, N., 2015. Variable input parameter influence on river corridor prediction. Proceedings of the ICE-Water Management 168 (5), 199–209. https://doi.org/10.1680/wama.13.00114.